

# Quantum theory of the third-order nonlinear electrodynamic effects of graphene

S. A. Mikhailov\*

*Institute of Physics, University of Augsburg, D-86135 Augsburg, Germany*

(Dated: May 13, 2019)

The linear energy dispersion of graphene electrons leads to a strongly nonlinear electromagnetic response of this material. We develop a general quantum theory of the third-order nonlinear local dynamic conductivity of graphene  $\sigma_{\alpha\beta\gamma\delta}(\omega_1, \omega_2, \omega_3)$ , which describes its nonlinear response to a uniform electromagnetic radiation. The derived analytical formulas describe a large number of different nonlinear phenomena such as the third harmonic generation, the four wave mixing, the saturable absorption, the second harmonic generation stimulated by a dc electric current, etc., which may be used in different terahertz and optoelectronic devices.

PACS numbers: 78.67.Wj, 42.65.Ky, 73.50.Fq

## Contents

<b>I. Introduction</b>	2
A. Brief overview of the problem	2
B. Overview of results	3
<b>II. Electronic spectrum, wave functions and matrix elements</b>	3
A. Tight binding energy and wave functions	3
B. Matrix elements	5
1. Matrix element of the exponential function	5
2. Matrix element of the velocity	6
<b>III. Linear response of graphene</b>	6
A. Preliminary remarks	6
B. Density matrix	7
C. Current density	7
D. First-order conductivity	8
<b>IV. Nonlinear (third-order) response of graphene</b>	9
A. Density matrix and the third-order current	9
B. Third-order conductivity	12
1. (3/0) contribution	12
2. (2/1) contribution	13
3. (1/2) contribution	14
4. (0/3) contribution	14
C. Summary of the third-order conductivity contributions	15
<b>V. Limiting cases</b>	16
A. Microwave/terahertz response of doped graphene, $\hbar\omega \lesssim 2E_F$	16
B. Optical response of intrinsic graphene, $\hbar\omega \gg 2E_F$	18
C. Resonances at $\hbar\omega \simeq 2E_F$	19
D. Logarithmic feature at $\hbar\omega \simeq 2E_F/3$	20
<b>VI. Third-order response to a monochromatic excitation</b>	21
A. Third harmonic generation, linear polarization	21
1. Third-order conductivity	21
2. Emitted power density at the third harmonic	22
B. Third harmonic generation, elliptic polarization	24
C. Third-order response at the incident-wave frequency: the absorption saturation	24
<b>VII. dc current induced second harmonic generation</b>	26

<b>VIII. Summary and Conclusions</b>	27
<b>A. Some useful formulas</b>	28
<b>B. Transformation of formulas (55) and (56)</b>	28
1. Transformation of the (1/2) term	28
2. Transformation of the (0/3) term	29
<b>References</b>	30

## I. INTRODUCTION

### A. Brief overview of the problem

Electrodynamic properties of graphene have attracted considerable attention in recent years<sup>1–4</sup>. Microwave and optical response, plasma and cyclotron resonances, nonlinear electromagnetic properties have been investigated both theoretically and experimentally in many research groups in the world<sup>5–17</sup>. Special interest to these topics is generated by the opportunity to use many of these fundamental phenomena for microwave-, terahertz- and optoelectronic applications<sup>2,4,18</sup>.

The most distinctive feature of graphene is the linear energy dispersion of its quasi-particles, electrons and holes,  $E_{\pm}(\mathbf{p}) = \pm v_F |\mathbf{p}|$ . It was theoretically predicted<sup>19</sup> and then experimentally confirmed<sup>20,21</sup>, that due to this property graphene should demonstrate strongly nonlinear electromagnetic behavior. Physically this can be understood as follows<sup>19</sup>. Assume that a particle with the linear spectrum is placed in the uniform external electric field  $\mathbf{E}(t) = \mathbf{E}_0 \cos \omega t$ . According to Newton equations of motion its momentum will oscillate as  $\mathbf{p}(t) \propto \sin \omega t$ , while the velocity  $\mathbf{v}(t) = \partial E / \partial \mathbf{p} \propto \mathbf{p}(t) / |\mathbf{p}(t)|$ , as well as the current  $\mathbf{j}(t)$ , which are *not* proportional to the momentum, will be strongly nonlinear functions of  $\mathbf{p}(t)$  and will therefore contain higher frequency harmonics,

$$j(t) \propto v(t) \propto \text{sgn}(\sin \omega t) \propto \sin \omega t + \frac{1}{3} \sin 3\omega t + \dots \quad (1)$$

In other words, since graphene electrons have no mass and can move in any direction only with the velocity  $v_F \approx 10^8$  cm/s, at the return points they have to instantaneously change their velocity from  $+10^8$  cm/s to  $-10^8$  cm/s which is accompanied by a strong acceleration and leads to emission of electromagnetic radiation. The nonlinear electrodynamic phenomena in graphene have been further studied in Refs.<sup>22–34</sup> (theory) and in Refs.<sup>35–46</sup> (experiment).

In most so far published theoretical publications the nonlinear (third-order) electromagnetic response of graphene was studied in the quasiclassical approximation, using the Boltzmann kinetic approach. Such a theory takes into account only the *intra*-band oscillations of the graphene electrons, which is valid at low (microwave/terahertz) frequencies  $\hbar\omega \lesssim 2E_F$ , where  $\omega$  is the radiation frequency,  $E_F \equiv |\mu|$  is the Fermi energy and  $\mu$  is the chemical potential. At higher (infrared, optical) frequencies the *inter*-band quantum transitions between the electron and hole bands should be taken into account and a quantum theory is needed. Recently, we have published<sup>28</sup> our first results of such a theory, having analytically calculated the third-order local dynamic conductivity of graphene  $\sigma_{\alpha\beta\gamma\delta}^{(3)}(\omega, \omega, \omega)$  which describes its response at the frequency  $3\omega$  to a monochromatic radiation with the frequency  $\omega = 2\pi f$  (the third harmonic generation). It was shown that the intra-band contribution to the third-harmonic effect strongly falls down with the frequency  $\omega$ , but at  $\hbar\omega \approx 2E_F$  one observes a strong resonance due to the inter-band transitions. This leads to a strong third-harmonic signal at the frequency  $f \approx E_F / \pi\hbar = v_F \sqrt{n_s / \pi}$  which can be tuned by the gate voltage; here  $n_s$  is the 2D electron density and  $v_F \approx 10^8$  cm/s is the Fermi velocity in graphene. This result is very interesting for different opto-electronic applications.

In this paper we develop a *general* quantum theory of the third-order nonlinear electromagnetic response of graphene. We calculate the third-order local dynamic conductivity  $\sigma_{\alpha\beta\gamma\delta}^{(3)}(\omega_1, \omega_2, \omega_3)$  which describes the graphene response to an external electric field with an arbitrary time dependence. Apart from the third-harmonic generation, these results describe a large number of other physical effects such as the four wave mixing, the saturable absorption, dc current stimulated second harmonic generation, response to a pulsed excitation and so on. Since the theory takes into account both the intra- and inter-band quantum transitions it is applicable at all frequencies from radiowaves up to visible light.

It should be noticed that results of calculations of the third conductivity  $\sigma_{\alpha\beta\gamma\delta}^{(3)}(\omega_1, \omega_2, \omega_3)$  have been recently reported by Cheng et al.<sup>32–34</sup>. These authors used the same starting equations but got results which differ from ours. Due to extreme complexity of the problem (it will be seen in subsequent sections) it is very difficult to find specific

reasons for the disagreement. However, in some special cases, in particular, in the high-frequency limit  $\hbar\omega_j \gg 2E_F$  ( $j = 1, 2, 3$ ) a direct comparison of results is possible. Such a comparison shows that several important terms which appear in our expression for  $\sigma_{\alpha\beta\gamma\delta}^{(3)}(\omega_1, \omega_2, \omega_3)$  are missing in the theory of Refs.<sup>32–34</sup>, see Eq. (109) and a discussion after it in Section V B for details. In some other places we also discuss specific disagreements between our results and those of Refs.<sup>32–34</sup> (see, e.g., the end of Section V).

## B. Overview of results

The paper contains technically complicated analytical calculations. To give the interested reader an opportunity to follow them we describe our solution in sufficient details. For those who wants to see only the results we give here a brief overview of how the paper is organized and where to find the main results of the work.

We describe the spectrum and the wave functions of graphene electrons in the tight-binding approximation. The corresponding formulas are introduced in Section II. Matrix elements of some operators needed in the rest of the paper are also calculated there.

In Section III the linear response of graphene<sup>6–8</sup> is discussed. Expressions for the first-order conductivity  $\sigma_{\alpha\beta}^{(1)}(\omega)$  are presented in Eqs. (43) – (47) and in Figure 2. These results are used then in Section VI C.

Section IV contains the main result of this work. Here we give a detailed derivation of the third conductivity  $\sigma_{\alpha\beta\gamma\delta}^{(3)}(\omega_1, \omega_2, \omega_3)$  and discuss different contributions (coming from different products of intra- and inter-band matrix elements) to it. A summary of (analytical) results for  $\sigma_{\alpha\beta\gamma\delta}^{(3)}(\omega_1, \omega_2, \omega_3)$  can be found in Eqs. (89) – (95) in Section IV C.

In Sections V – VII we analyze our results in different limiting cases. Section V is devoted to the study of important limiting cases: we consider regimes of low (radio-microwave-terahertz) frequencies in Section V A and high (infrared-optical) frequencies in Section V B. Here we also give estimates of numerical values of the nonlinear parameters of graphene ( $\sigma^{(3)}$  and  $\chi^{(3)}$ ) in different frequency regimes (notice that all these estimates are valid for an isolated graphene layer; for a graphene layer immersed in a dielectric/metallic structure the corresponding numbers can be different). We also consider the behavior and numerical values of the third conductivity near the resonance at  $\hbar\omega \simeq 2E_F$  (Section V C) and near the (weak) logarithmic feature at  $\hbar\omega \simeq 2E_F/3$  (Section V D).

In Section VI we investigate the graphene response to an external monochromatic radiation with the frequency  $\omega$ . We consider the  $3\omega$ -response (the third harmonic generation) at the linear and elliptic polarization of the incident wave (Sections VI A and VI B, Figures 4–6) and the  $\omega$ -response (Section VI C, Figures 7–9) which manifests itself as the absorption saturation in strong electric fields of the incident wave.

Since graphene is a centrosymmetric material the observation of the second-order effects in it (in the uniform infinite sample) is forbidden. This prohibition can be removed if the central symmetry is violated, e.g., by a dc current flowing in the layer in a certain direction. In Section VII we investigate this situation and calculate the  $2\omega$ -response of graphene (the second-harmonic generation, Figure 10) in the presence of a dc current in the system.

Finally, in Section VIII we give a brief summary of all obtained results and discuss the main conclusions from this work. In Appendix some useful formulas are collected and some details of calculations are further discussed.

## II. ELECTRONIC SPECTRUM, WAVE FUNCTIONS AND MATRIX ELEMENTS

### A. Tight binding energy and wave functions

The carbon atoms in graphene occupy a 2D plane ( $z = 0$ ) and are arranged in a honey-comb lattice, Fig. 1a, composed out of two triangular sublattices shifted by a vector  $\mathbf{b}$  with respect to each other. All points of the first sublattice (black circles in Fig. 1a) are given by the vectors  $n_1\mathbf{a}_1 + n_2\mathbf{a}_2$  and those of the second sublattice (open circles) by  $n_1\mathbf{a}_1 + n_2\mathbf{a}_2 + \mathbf{b}$ , where  $n_1$  and  $n_2$  are integers. The basis vectors  $\mathbf{a}_1$ ,  $\mathbf{a}_2$  and the vector  $\mathbf{b}$  are chosen as shown in Fig. 1a,  $\mathbf{a}_1 = a(1/2, \sqrt{3}/2)$ ,  $\mathbf{a}_2 = a(-1/2, \sqrt{3}/2)$ ,  $\mathbf{b} = a(0, 1/\sqrt{3})$ , where  $a = |\mathbf{a}_1| = |\mathbf{a}_2| = 2.46$  Å is the lattice constant.

The carbon atom has four electrons on its outer shell. Three of them, so called  $\sigma$ -electrons, form chemical bonds with their neighbors. The fourth ( $\pi$ -) electron moves in the periodic potential of the honey-comb lattice,

$$U(\mathbf{r}, z) = \sum_{\mathbf{a}} [U_a(\mathbf{r} - \mathbf{a}, z) + U_a(\mathbf{r} - \mathbf{a} - \mathbf{b}, z)], \quad (2)$$

where  $U_a$  is the atomic potential,  $\mathbf{r} = (x, y)$  is a two-dimensional vector, and the sum is taken over all  $\mathbf{a}$  vectors of the lattice. We will describe its motion within the tight-binding approximation. Within this approach the single-particle

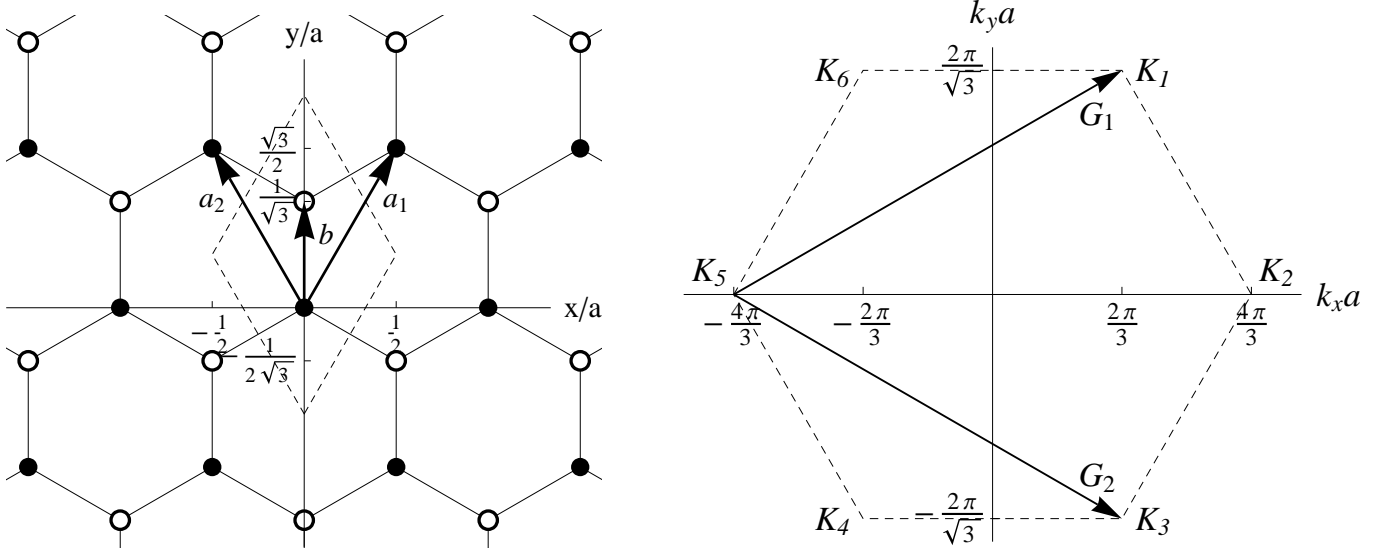


FIG. 1: Left: The honeycomb lattice of graphene;  $\mathbf{a}_1 = a(1/2, \sqrt{3}/2)$ ,  $\mathbf{a}_2 = a(-1/2, \sqrt{3}/2)$ ,  $\mathbf{b} = a(0, 1/\sqrt{3})$ ,  $a$  is the lattice constant. Right: The Brillouin zone of graphene;  $\mathbf{G}_1 = (2\pi/a)(1, 1/\sqrt{3})$ ,  $\mathbf{G}_2 = (2\pi/a)(1, -1/\sqrt{3})$ ,  $|\mathbf{G}_1| = |\mathbf{G}_2| = G = 4\pi/(\sqrt{3}a)$ ;  $\mathbf{K}_1 = -\mathbf{K}_4 = (2\pi/a)(1/3, 1/\sqrt{3})$ ,  $\mathbf{K}_2 = -\mathbf{K}_5 = (2\pi/a)(2/3, 0)$ ,  $\mathbf{K}_3 = -\mathbf{K}_6 = (2\pi/a)(1/3, -1/\sqrt{3})$ . Dashed lines show the boundaries of the elementary cell in the direct and reciprocal space.

Hamiltonian is

$$\hat{H}_0 = \frac{\hat{\mathbf{p}}^2}{2m} + \frac{\hat{p}_z^2}{2m} + U(\mathbf{r}, z), \quad (3)$$

where  $\hat{\mathbf{p}} = -i\hbar(\partial_x, \partial_y)$  and  $m$  is the free electron mass. Following the standard procedure of the tight binding approximation and assuming only the nearest neighbors interaction we find the energy

$$E_{l\mathbf{k}} = (-1)^l t |\mathcal{Z}_{\mathbf{k}}|, \quad (4)$$

and the wave functions of the Hamiltonian (3)

$$\Psi_{l\mathbf{k}}(\mathbf{r}, z) = |l\mathbf{k}\rangle = \frac{1}{\sqrt{S}} e^{i\mathbf{k}\cdot\mathbf{r}} u_{l\mathbf{k}}(\mathbf{r}, z), \quad (5)$$

where

$$u_{l\mathbf{k}}(\mathbf{r}, z) = |l\mathbf{k}\rangle = \sqrt{\frac{A}{2}} \sum_{\mathbf{a}} e^{-i\mathbf{k}\cdot(\mathbf{r}-\mathbf{a})} [(-1)^l \zeta_{\mathbf{k}} \psi_a(\mathbf{r} - \mathbf{a}, z) + \psi_a(\mathbf{r} - \mathbf{a} - \mathbf{b}, z)] \quad (6)$$

is the Bloch factor,  $l = 1, 2$  is the band index,  $\mathbf{k} = (k_x, k_y)$ ,  $t$  is the transfer integral (in graphene  $t \approx 3$  eV),  $S$  and  $A$  are the areas of the sample and of the elementary cell, respectively, and  $\psi_a$  is the atomic wave function. The functions  $\mathcal{Z}_{\mathbf{k}}$  and  $\zeta_{\mathbf{k}}$  in (4), (6) are defined as

$$\mathcal{Z}_{\mathbf{k}} = 1 + e^{i\mathbf{k}\cdot\mathbf{a}_1} + e^{i\mathbf{k}\cdot\mathbf{a}_2} = 1 + 2 \cos(k_x a/2) e^{i\sqrt{3}k_y a/2}, \quad (7)$$

$$\zeta_{\mathbf{k}} = \mathcal{Z}_{\mathbf{k}}/|\mathcal{Z}_{\mathbf{k}}| = e^{i\Phi_{\mathbf{k}}}, \quad (8)$$

where  $\Phi_{\mathbf{k}}$  is the phase of the complex function  $\mathcal{Z}_{\mathbf{k}}$ . They satisfy the relations

$$\mathcal{Z}_{-\mathbf{k}} = \mathcal{Z}_{\mathbf{k}}^*, \quad \mathcal{Z}_{\mathbf{k}+\mathbf{G}} = \mathcal{Z}_{\mathbf{k}}, \quad \zeta_{-\mathbf{k}} = \zeta_{\mathbf{k}}^*, \quad \zeta_{\mathbf{k}+\mathbf{G}} = \zeta_{\mathbf{k}}, \quad (9)$$

where  $\mathbf{G}$  are the 2D reciprocal lattice vectors which can be chosen as shown in Fig. 1b,  $\mathbf{G}_1 = (2\pi/a)(1, 1/\sqrt{3})$ ,  $\mathbf{G}_2 = (2\pi/a)(1, -1/\sqrt{3})$ . The energy  $E_{l\mathbf{k}}$  and the wave functions  $|l\mathbf{k}\rangle$  are periodic in  $\mathbf{k}$ -space,  $E_{l,\mathbf{k}+\mathbf{G}} = E_{l\mathbf{k}}$  and  $|l, \mathbf{k} + \mathbf{G}\rangle = |l\mathbf{k}\rangle$ . The functions (5) and (6) are normalized as follows

$$\langle l'\mathbf{k}' | l\mathbf{k} \rangle \equiv \int_S d\mathbf{r} \int_{-\infty}^{\infty} dz \Psi_{l'\mathbf{k}'}^*(\mathbf{r}, z) \Psi_{l\mathbf{k}}(\mathbf{r}, z) = \delta_{\mathbf{k}\mathbf{k}'} \delta_{ll'}, \quad (10)$$

$$(l'k|lk) \equiv \frac{1}{A} \int_A d\mathbf{r} \int_{-\infty}^{\infty} dz u_{l'k}^*(\mathbf{r}, z) u_{lk}(\mathbf{r}, z) = \delta_{ll'}. \quad (11)$$

Near the Dirac points, at the corners of the hexagon shaped Brillouin zone  $\mathbf{k} = \mathbf{K}_j$  ( $j = 1, \dots, 6$  is the valley index, Fig. 1b), the function  $\mathcal{Z}_k$  assumes the form

$$\mathcal{Z}_k^j \approx -\frac{\sqrt{3}a}{2} \left[ (-1)^j \tilde{k}_x^j + i \tilde{k}_y^j \right], \quad \tilde{\mathbf{k}}_j = \mathbf{k} - \mathbf{K}_j, \quad (12)$$

where  $\mathbf{K}_1 = -\mathbf{K}_4 = (2\pi/a)(1/3, 1/\sqrt{3})$ ,  $\mathbf{K}_2 = -\mathbf{K}_5 = (2\pi/a)(2/3, 0)$ ,  $\mathbf{K}_3 = -\mathbf{K}_6 = (2\pi/a)(1/3, -1/\sqrt{3})$ . The energy (4) and the function  $\zeta_k$  are then (at  $|\tilde{\mathbf{k}}_j|a \ll 1$ )

$$E_{lk}^j = (-1)^l \frac{t\sqrt{3}a}{2} |\tilde{\mathbf{k}}_j| \equiv (-1)^l v_F \hbar |\tilde{\mathbf{k}}_j|, \quad (13)$$

$$\zeta_{\mathbf{k}j} = -\frac{(-1)^j \tilde{k}_x^j + i \tilde{k}_y^j}{|\tilde{\mathbf{k}}_j|} = (-1)^{j+1} e^{(-1)^j i \varphi_{\mathbf{k}}}, \quad (14)$$

where the effective (Fermi) velocity is  $v_F = t\sqrt{3}a/2\hbar \approx 10^8$  cm/s, and  $\varphi_{\mathbf{k}}$  is the polar angle of the vector  $\tilde{\mathbf{k}}$ ,  $\tilde{\mathbf{k}} = (\tilde{k}_x, \tilde{k}_y) = \tilde{k}(\cos \varphi_{\mathbf{k}}, \sin \varphi_{\mathbf{k}})$ .

In typical graphene structures the chemical potential  $\mu$  lies in the vicinity of Dirac points,  $|\mu| \ll t$ . In this paper we will assume that the energy of the photon is also small as compared to the overlap integral  $t$ ,  $\hbar\omega \ll t$ . Under these conditions the energy and the wave-functions of electrons can be described with the help of formulas (13) and (14) valid in the vicinity of Dirac points.

## B. Matrix elements

To calculate the system response in subsequent chapters we will need some matrix elements with the tight-binding functions (5).

### 1. Matrix element of the exponential function

Consider the matrix element  $\langle lk|e^{i\mathbf{q}\cdot\mathbf{r}}|l'k'\rangle$  of the exponential function  $e^{i\mathbf{q}\cdot\mathbf{r}}$ . Assuming as above that the neighboring wave functions do not overlap we get

$$\langle lk|e^{i\mathbf{q}\cdot\mathbf{r}}|l'k'\rangle = \delta_{\mathbf{k}, \mathbf{k}' + \mathbf{q}} \frac{1}{2} \left[ 1 + (-1)^{l'+l} \zeta_{\mathbf{k}}^* \zeta_{\mathbf{k}-\mathbf{q}} \right]. \quad (15)$$

The matrix element is nonzero only at  $\mathbf{k} = \mathbf{k}' + \mathbf{q}$ . Eq. (15) is valid in the whole Brillouin zone and at arbitrary values of  $\mathbf{q}$ . Since we aim to calculate the local ( $\mathbf{q} = \mathbf{0}$ ) conductivity  $\sigma_{\alpha\beta\gamma\delta}^{(3)}(\omega_1, \omega_2, \omega_3)$  we will need these matrix elements at  $\mathbf{q} \rightarrow \mathbf{0}$ , however, the terms linear in  $q$  must be kept. Then the matrix element (15) assumes the form

$$\langle lk|e^{i\mathbf{q}\cdot\mathbf{r}}|l'k'\rangle_{\mathbf{q} \rightarrow \mathbf{0}} \approx \delta_{l'l} \delta_{\mathbf{k}, \mathbf{k}' + \mathbf{q}} + (1 - \delta_{l'l}) \delta_{\mathbf{k}, \mathbf{k}'} \frac{1}{2} q_{\alpha} \eta_{\mathbf{k}}^{\alpha} \quad (16)$$

where

$$\eta_{\mathbf{k}}^{\alpha} = \frac{\partial \zeta_{\mathbf{k}}}{\partial k_{\alpha}} \zeta_{\mathbf{k}}^* = i \frac{\partial \Phi_{\mathbf{k}}}{\partial k_{\alpha}}. \quad (17)$$

In the first term in (16) ( $l = l'$ , the intra-band matrix element) the  $\mathbf{q}$ -correction in the Kronecker symbol is essential; as will be seen below it leads to the intra-band contributions to the conductivities  $\sigma_{\alpha\beta}^{(1)}(\omega)$  and  $\sigma_{\alpha\beta\gamma\delta}^{(3)}(\omega_1, \omega_2, \omega_3)$ . In the second term ( $l \neq l'$ , the inter-band matrix element) we have already the prefactor  $q_{\alpha}$ , therefore  $\delta_{\mathbf{k}, \mathbf{k}' + \mathbf{q}}$  can be replaced by  $\delta_{\mathbf{k}, \mathbf{k}'}$ .

Near the Dirac points  $j = 1$  and  $j = 2$  the function  $\zeta_{\mathbf{k}}$  is given by Eq. (14). Substituting this in Eq. (17) we get

$$\eta_{\mathbf{k}j}^{\alpha} = \mp i \frac{\partial \varphi_{\mathbf{k}}}{\partial k_{\alpha}} = \pm \frac{i}{k^2} \epsilon_{\alpha\beta} k_{\beta}, \quad (18)$$

where the upper (lower) sign corresponds to  $j = 1$  ( $j = 2$ ) and the two-dimensional Levi-Civita symbol is defined in (A1). Notice that the more general formula (17) is valid in the whole Brillouin zone.

## 2. Matrix element of the velocity

Another quantity that we will need below is the diagonal in  $\mathbf{k}$  ( $\mathbf{k} = \mathbf{k}'$ ) matrix element of the velocity operator  $\langle l\mathbf{k}|\hat{\mathbf{v}}|l'\mathbf{k}\rangle$ , where  $\hat{\mathbf{v}} = \hat{\mathbf{p}}/m$  (here  $m$  is the free electron mass). To find it, consider the matrix element  $\langle l\mathbf{k}|[\hat{H}_0, e^{i\mathbf{q}\cdot\mathbf{r}}]|l'\mathbf{k}'\rangle$ . On the one hand it equals

$$\langle l\mathbf{k}|[\hat{H}_0, e^{i\mathbf{q}\cdot\mathbf{r}}]|l'\mathbf{k}'\rangle = (E_{l\mathbf{k}} - E_{l'\mathbf{k}'})\langle l\mathbf{k}|e^{i\mathbf{q}\cdot\mathbf{r}}|l'\mathbf{k}'\rangle. \quad (19)$$

On the other hand

$$[\hat{H}_0, e^{i\mathbf{q}\cdot\mathbf{r}}] = \frac{1}{2m}[\hat{\mathbf{p}}^2, e^{i\mathbf{q}\cdot\mathbf{r}}] = \frac{\hbar\mathbf{q}}{2} \cdot (\hat{\mathbf{v}}e^{i\mathbf{q}\cdot\mathbf{r}} + e^{i\mathbf{q}\cdot\mathbf{r}}\hat{\mathbf{v}}), \quad (20)$$

so that

$$\frac{\hbar\mathbf{q}}{2} \cdot \langle l\mathbf{k}|\hat{\mathbf{v}}e^{i\mathbf{q}\cdot\mathbf{r}} + e^{i\mathbf{q}\cdot\mathbf{r}}\hat{\mathbf{v}}|l'\mathbf{k}'\rangle = (E_{l\mathbf{k}} - E_{l'\mathbf{k}'})\langle l\mathbf{k}|e^{i\mathbf{q}\cdot\mathbf{r}}|l'\mathbf{k}'\rangle. \quad (21)$$

Now consider small values of  $\mathbf{q}$  and two different cases,  $l = l'$  and  $l \neq l'$ . If  $l = l'$ , the matrix element of the exponential function in the right-hand side of (21) is given by  $\langle l\mathbf{k}|e^{i\mathbf{q}\cdot\mathbf{r}}|l\mathbf{k}'\rangle \approx \delta_{\mathbf{k},\mathbf{k}'+\mathbf{q}}$ , the energy difference is  $E_{l\mathbf{k}} - E_{l\mathbf{k}-\mathbf{q}} = q_\alpha \partial E_{l\mathbf{k}} / \partial k_\alpha$ , and we get, keeping only the lowest terms in  $q$ :

$$q_\alpha \left( \hbar \langle l\mathbf{k}|\hat{v}_\alpha|l\mathbf{k}\rangle - \frac{\partial E_{l\mathbf{k}}}{\partial k_\alpha} \right) = 0. \quad (22)$$

If  $l \neq l'$ , the matrix element of the exponential function in the right-hand side of (21) is proportional to  $q_\alpha \eta_{\mathbf{k}}^\alpha$ , and we get, keeping again only the lowest terms in  $q$ :

$$q_\alpha \left( 2\hbar \langle l\mathbf{k}|\hat{v}_\alpha|l'\mathbf{k}\rangle - (E_{l\mathbf{k}} - E_{l'\mathbf{k}})\eta_{\mathbf{k}}^\alpha \right) = 0. \quad (23)$$

Since the direction of the vector  $\mathbf{q}$  in both formulas (22) and (23) is arbitrary, the terms in parenthesis must vanish. Thus we get for the intra- and inter-band matrix elements of the velocity

$$\langle l\mathbf{k}|\hat{v}_\alpha|l\mathbf{k}\rangle = \frac{1}{\hbar} \frac{\partial E_{l\mathbf{k}}}{\partial k_\alpha}, \quad l = l', \quad (24)$$

$$\langle l\mathbf{k}|\hat{v}_\alpha|l'\mathbf{k}\rangle = \frac{E_{l\mathbf{k}} - E_{l'\mathbf{k}}}{2\hbar} \eta_{\mathbf{k}}^\alpha, \quad l \neq l'. \quad (25)$$

The formulas (24) and (25) are valid not only near the Dirac points but in the whole Brillouin zone. Near the Dirac point one can use (13) for the energy and (18) for the  $\eta_{\mathbf{k}}^\alpha$ -function.

## III. LINEAR RESPONSE OF GRAPHENE

### A. Preliminary remarks

Our ultimate goal is to calculate the current response  $\mathbf{j}(t)$  of a uniform graphene layer to an external *uniform* electric field  $\mathbf{E}(t)$  parallel to it. The field is assumed to have an arbitrary time dependence and be presented by Fourier expansion

$$\mathbf{E}(t) = \int_{-\infty}^{\infty} d\omega \mathbf{E}_\omega e^{-i\omega t}. \quad (26)$$

The current response  $\mathbf{j}(t)$  will have to be calculated in up to the third order in the electric field  $\mathbf{E}$ .

The external ac electric field can be included in the Hamiltonian of the system in two ways, using a vector or a scalar potential  $\phi(\mathbf{r}, t)$ . We choose the second option and write the Hamiltonian in the form

$$\hat{H} = \hat{H}_0 + \hat{H}_1 = \hat{H}_0 - e\phi(\mathbf{r}, t), \quad (27)$$

where the potential can be expanded in the Fourier integral over time,

$$\phi(\mathbf{r}, t) = \int_{-\infty}^{\infty} d\omega \phi_{\omega}(\mathbf{r}) e^{-i\omega t + \gamma t}, \quad \gamma \rightarrow 0. \quad (28)$$

Notice that at the moment we assume  $\phi(\mathbf{r}, t)$  to be space-dependent,

$$\phi_{\omega}(\mathbf{r}) = \sum_{\mathbf{q}} \phi_{\mathbf{q}\omega} e^{i\mathbf{q} \cdot \mathbf{r}}, \quad (29)$$

where the sums are taken over discretized  $\mathbf{q}$  values, and the transition from the sum to the integral is performed using the usual rule

$$\sum_{\mathbf{q}} (\dots) \rightarrow \frac{S}{(2\pi)^2} \int \int (\dots) d\mathbf{q}. \quad (30)$$

This has to be done since the field is proportional to the gradient of the potential,  $\mathbf{E}(\mathbf{r}, t) = -\nabla\phi(\mathbf{r}, t)$ , and its Fourier component is  $\mathbf{E}_{\mathbf{q}\omega} = -i\mathbf{q}\phi_{\mathbf{q}\omega}$ . In order to calculate the local ( $\mathbf{q} \rightarrow \mathbf{0}$ ) conductivities  $\sigma^{(1)}$  and  $\sigma^{(3)}$  we have, first, to find the current response at a finite wave-vector and then take the limit  $\mathbf{q} \rightarrow \mathbf{0}$  in the final formulas. The factor  $\mathbf{q}\phi_{\mathbf{q}\omega}$  should however be kept finite in the limiting procedure.

In this Section we discuss this process in sufficient detail for the linear response problem. The nonlinear response is then treated in Section IV.

## B. Density matrix

The system response to the potential (28) is described by Liouville equation for the density matrix  $\hat{\rho}$

$$i\hbar \frac{\partial \hat{\rho}}{\partial t} = [\hat{H}_0 + \hat{H}_1, \hat{\rho}]. \quad (31)$$

The unperturbed Hamiltonian  $\hat{H}_0$  and the density matrix  $\hat{\rho}_0$  satisfy the eigen-value equations

$$\hat{H}_0|\lambda\rangle = E_{\lambda}|\lambda\rangle, \quad \hat{\rho}_0|\lambda\rangle = f_{\lambda}|\lambda\rangle, \quad (32)$$

where  $|\lambda\rangle = |l\mathbf{k}\sigma\rangle$  (we have added the spin variable  $\sigma$ ) and  $f_{\lambda} = f_{l\mathbf{k}}$  is the Fermi distribution function

$$f_{l\mathbf{k}} = \left( 1 + \exp \frac{E_{l\mathbf{k}} - \mu}{T} \right)^{-1}. \quad (33)$$

Expanding the density matrix in powers of the electric field,  $\hat{\rho} = \hat{\rho}_0 + \hat{\rho}_1 + \hat{\rho}_2 + \hat{\rho}_3 + \dots$ ,  $\hat{\rho}_n \propto E^n$ , and solving the Liouville equation in the first order we get

$$\langle \lambda | \rho_1 | \lambda' \rangle_t = \int_{-\infty}^{\infty} d\omega \frac{f_{\lambda'} - f_{\lambda}}{E_{\lambda'} - E_{\lambda} + \hbar(\omega + i\gamma)} \langle \lambda | h_{\omega} | \lambda' \rangle e^{-i\omega t + \gamma t}, \quad (34)$$

where  $h_{\omega} \equiv h_{\omega}(\mathbf{r}) = -e\phi_{\omega}(\mathbf{r})$  and the subscript  $t$  indicates that the density matrix elements  $\langle \lambda | \rho_1 | \lambda' \rangle_t$  depend on time [the integrand in (34), apart from the exponential function, will then be denoted as  $\langle \lambda | \rho_1 | \lambda' \rangle_{\omega}$ ]. The quantity  $\gamma$  introduced in (28) shifts the pole in (34) into the complex plane thus helping to avoid unphysical divergences of the integrals; it can be, roughly, associated with the effective (phenomenological) electron scattering time.

## C. Current density

The two-dimensional current density is calculated according to the formula

$$\mathbf{j}(\mathbf{r}_0, t) = -\frac{e}{2} \sum_{\lambda\lambda'} \langle \lambda' | \{ \hat{\mathbf{v}} \delta(\mathbf{r}_0 - \mathbf{r}) \}_{+} | \lambda \rangle \langle \lambda | \rho | \lambda' \rangle_t, \quad (35)$$

where  $\{\dots\}_+$  means the anticommutator. In the first order we get for the  $\omega$ -Fourier component of the current

$$\mathbf{j}_\omega(\mathbf{r}_0) = \frac{e^2}{2} \sum_{\lambda\lambda'} \langle \lambda' | \{\hat{\mathbf{v}}\delta(\mathbf{r}_0 - \mathbf{r})\}_+ | \lambda \rangle \frac{f_{\lambda'} - f_\lambda}{E_{\lambda'} - E_\lambda + \hbar(\omega + i\gamma)} \langle \lambda | \phi_\omega(\mathbf{r}) | \lambda' \rangle. \quad (36)$$

Now we expand the potential in Fourier integral in  $\mathbf{q}$ , Eq. (29), and use the Dirac function representation

$$\delta(\mathbf{r}_0 - \mathbf{r}) = \frac{1}{S} \sum_{\tilde{\mathbf{q}}} e^{i\tilde{\mathbf{q}} \cdot (\mathbf{r}_0 - \mathbf{r})}. \quad (37)$$

Then we get

$$\mathbf{j}_{\tilde{\mathbf{q}}\omega} = \frac{e^2}{2S} \sum_{\mathbf{q}} \phi_{\mathbf{q}\omega} \sum_{\lambda\lambda'} \langle \lambda' | \{\hat{\mathbf{v}}, e^{-i\tilde{\mathbf{q}} \cdot \mathbf{r}}\}_+ | \lambda \rangle \frac{f_{\lambda'} - f_\lambda}{E_{\lambda'} - E_\lambda + \hbar(\omega + i\gamma)} \langle \lambda | e^{i\mathbf{q} \cdot \mathbf{r}} | \lambda' \rangle. \quad (38)$$

The formula (38) is general and valid at arbitrary  $\mathbf{q}$ . In the limit  $\mathbf{q} \rightarrow \mathbf{0}$  we can simplify it, substituting the matrix element expansion (16), thus getting the intra-band (first term) and inter-band (second term) contributions to the current:

$$j_\omega^\alpha = \left[ \frac{ie^2 g_s}{\hbar(\omega + i\gamma)S} \sum_{l\mathbf{k}} \langle l\mathbf{k} | \hat{v}_\alpha | l\mathbf{k} \rangle \left( -\frac{\partial f_{l\mathbf{k}}}{\partial k_\beta} \right) + \frac{ie^2 g_s}{2S} \sum_{l\mathbf{k}} \langle \bar{l}\mathbf{k} | \hat{v}_\alpha | l\mathbf{k} \rangle \frac{f_{\bar{l}\mathbf{k}} - f_{l\mathbf{k}}}{E_{\bar{l}\mathbf{k}} - E_{l\mathbf{k}} + \hbar(\omega + i\gamma)} \eta_{\mathbf{k}}^\beta \right] E_\omega^\beta. \quad (39)$$

Here  $g_s = 2$  is the spin degeneracy factor,

$$E_\omega^\beta = \lim_{\mathbf{q} \rightarrow \mathbf{0}} E_{\mathbf{q}\omega}^\beta = \lim_{\mathbf{q} \rightarrow \mathbf{0}} \left( -iq_\beta \phi_{\mathbf{q}\omega} \right), \quad (40)$$

and we have introduced a designation  $\bar{l}$  which means *not*  $l$ , i.e.

$$\bar{l} = \begin{cases} 2, & \text{if } l = 1, \\ 1, & \text{if } l = 2. \end{cases} \quad (41)$$

Notice that the sums in (39) are taken over the whole Brillouin zone of graphene, therefore the valley degeneracy factor  $g_v = 2$  has not yet appeared in this expression.

#### D. First-order conductivity

The value in the parenthesis in (39) is the linear (first-order) local conductivity of graphene

$$\sigma_{\alpha\beta}^{(1)}(\omega) = \frac{ie^2 g_s}{\hbar(\omega + i\gamma)S} \sum_{l\mathbf{k}} \langle l\mathbf{k} | \hat{v}_\alpha | l\mathbf{k} \rangle \left( -\frac{\partial f_{l\mathbf{k}}}{\partial k_\beta} \right) + \frac{ie^2 g_s}{2S} \sum_{l\mathbf{k}} \langle \bar{l}\mathbf{k} | \hat{v}_\alpha | l\mathbf{k} \rangle \frac{f_{\bar{l}\mathbf{k}} - f_{l\mathbf{k}}}{E_{\bar{l}\mathbf{k}} - E_{l\mathbf{k}} + \hbar(\omega + i\gamma)} \eta_{\mathbf{k}}^\beta. \quad (42)$$

This quantity has been calculated in a number of publications, see e.g.<sup>6–8</sup>, therefore we do not discuss here further details of the integral calculations in (42). Assuming that the temperature is zero,  $T = 0$ , and taking into account that the main contribution to the sums over  $\mathbf{k}$  is given by the vicinity of Dirac points we get

$$\sigma_{\alpha\beta}^{(1)}(\omega) = \sigma_0^{(1)} \mathcal{S}_{\alpha\beta}^{(1)}(\Omega), \quad (43)$$

where

$$\sigma_0^{(1)} = \frac{e^2 g_s g_v}{16\hbar} = \frac{e^2}{4\hbar} \quad (44)$$

is the universal optical conductivity<sup>13,14</sup> and the dimensionless function

$$\mathcal{S}_{\alpha\beta}^{(1)}(\Omega) = \delta_{\alpha\beta} \left( \mathcal{S}_{\text{intra}}^{(1)}(\Omega) + \mathcal{S}_{\text{inter}}^{(1)}(\Omega) \right), \quad (45)$$

consists of two, intra-band and inter-band, contributions,

$$\mathcal{S}_{\text{intra}}^{(1)}(\Omega) = \frac{4}{\pi} \frac{i}{\Omega + i\Gamma}, \quad (46)$$

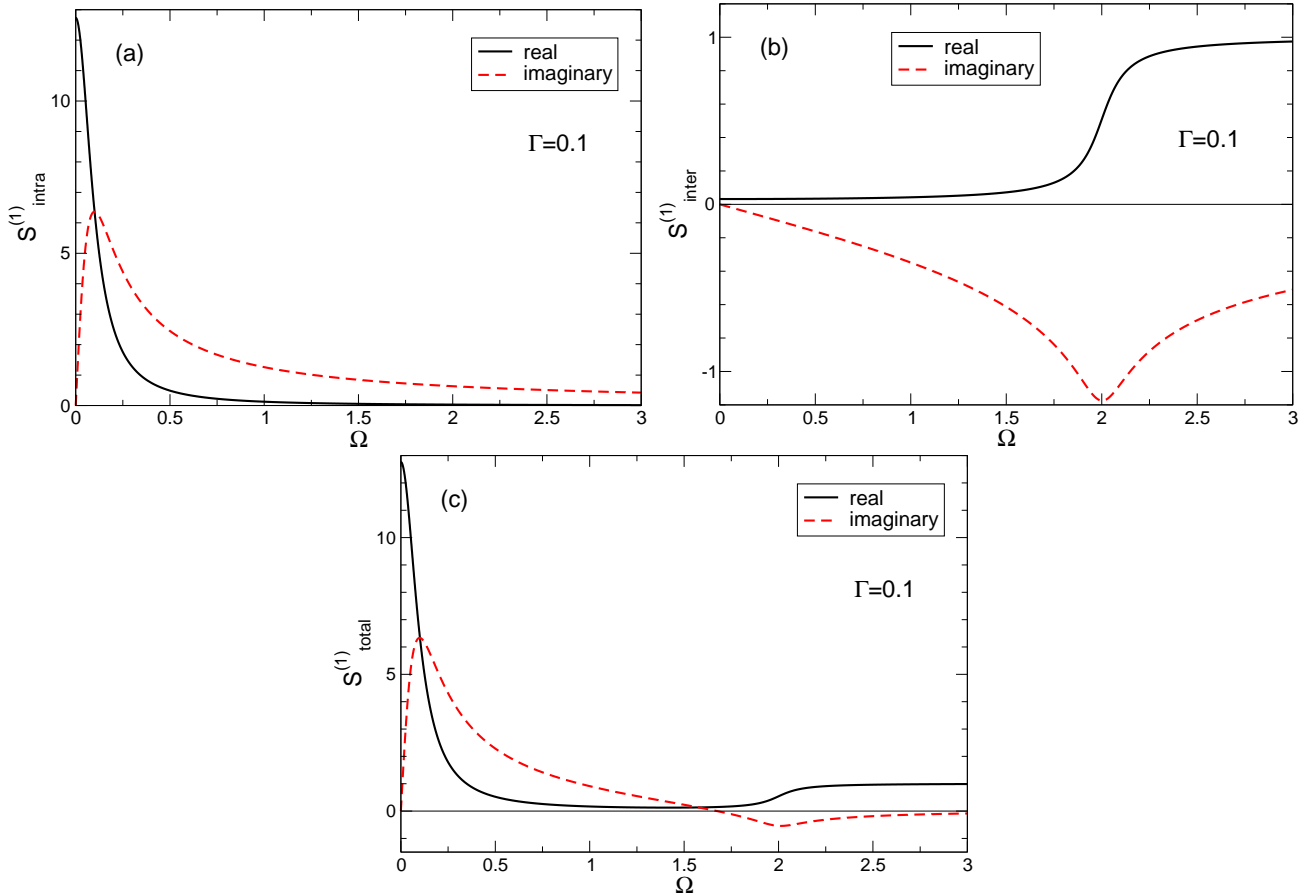


FIG. 2: (a) The intra-band (46), (b) inter-band (47), and (c) total conductivity of a single graphene layer as a function of the frequency  $\Omega = \hbar\omega/E_F$  at  $\Gamma = \hbar\gamma/E_F = 0.1$ .

$$S_{\text{inter}}^{(1)}(\Omega) = \frac{i}{\pi} \ln \frac{2 - (\Omega + i\Gamma)}{2 + (\Omega + i\Gamma)}. \quad (47)$$

We have introduced here two dimensionless parameters

$$\Omega = \frac{\hbar\omega}{|\mu|}, \quad \Gamma = \frac{\hbar\gamma}{|\mu|}. \quad (48)$$

The intra-band contribution (46) has the Drude form; the inter-band conductivity (47) has a step-like (logarithmic) feature at  $\hbar\omega \simeq 2E_F$  in its real (imaginary) part. At large frequencies  $\hbar\omega \gg 2E_F$  the conductivity assumes the universal value (44). Figure 2 shows the intra-band, inter-band and the total conductivity of graphene at  $\Gamma = 0.1$ .

#### IV. NONLINEAR (THIRD-ORDER) RESPONSE OF GRAPHENE

##### A. Density matrix and the third-order current

Now we need to calculate the next term in the expansion of the electric current in powers of the electric field. The second-order current response  $\propto \mathbf{E}^2(t)$  vanishes due to the central symmetry of graphene. In the third order in the perturbation (28) the solution of Liouville equation (31) can be written in the form

$$\begin{aligned} \langle \lambda | \rho_3 | \lambda' \rangle_t &= \int_{-\infty}^{\infty} d\omega_1 \int_{-\infty}^{\infty} d\omega_2 \int_{-\infty}^{\infty} d\omega_3 \frac{e^{-i(\omega_1 + \omega_2 + \omega_3 + 3i\gamma)t}}{E_{\lambda'} - E_{\lambda} + \hbar(\omega_1 + \omega_2 + \omega_3) + i\hbar 3\gamma} \sum_{\lambda'' \lambda'''} \langle \lambda | h_{\omega_3} | \lambda''' \rangle \langle \lambda''' | h_{\omega_2} | \lambda'' \rangle \langle \lambda'' | h_{\omega_1} | \lambda' \rangle \\ &\times \left[ \frac{1}{E_{\lambda'} - E_{\lambda'''} + \hbar(\omega_1 + \omega_2) + i2\hbar\gamma} \left( \frac{f_{\lambda'} - f_{\lambda''}}{E_{\lambda'} - E_{\lambda''} + \hbar\omega_1 + i\hbar\gamma} - \frac{f_{\lambda''} - f_{\lambda''''}}{E_{\lambda''} - E_{\lambda'''} + \hbar\omega_2 + i\hbar\gamma} \right) \right. \end{aligned}$$

$$- \frac{1}{E_{\lambda''} - E_{\lambda} + \hbar(\omega_2 + \omega_3) + i2\hbar\gamma} \left( \frac{f_{\lambda''} - f_{\lambda'''}}{E_{\lambda''} - E_{\lambda'''} + \hbar\omega_2 + i\hbar\gamma} - \frac{f_{\lambda'''} - f_{\lambda}}{E_{\lambda'''} - E_{\lambda} + \hbar\omega_3 + i\hbar\gamma} \right). \quad (49)$$

In order to find the current density in the third-order we should substitute Eq. (49) in the current definition (35),

$$\mathbf{j}^{(3)}(\mathbf{r}_0, t) = -\frac{e}{2} \sum_{\lambda\lambda'} \langle \lambda' | \{ \hat{\mathbf{v}}, \delta(\mathbf{r}_0 - \mathbf{r}) \}_+ | \lambda \rangle \langle \lambda | \rho_3 | \lambda' \rangle_t, \quad (50)$$

and calculate all (intra- and inter-band) contributions to it. This is a very complicated problem. Let us analyze it step by step.

First we notice that the current density (50)–(49) contains the product of three matrix elements of the type (15),

$$\langle \lambda | h_{\omega_3} | \lambda''' \rangle \langle \lambda''' | h_{\omega_2} | \lambda'' \rangle \langle \lambda'' | h_{\omega_1} | \lambda' \rangle \propto \sum_{\mathbf{q}_1 \mathbf{q}_2 \mathbf{q}_3} \phi_{\mathbf{q}_1 \omega_1} \phi_{\mathbf{q}_2 \omega_2} \phi_{\mathbf{q}_3 \omega_3} \langle \lambda | e^{i\mathbf{q}_3 \cdot \mathbf{r}_3} | \lambda''' \rangle \langle \lambda''' | e^{i\mathbf{q}_2 \cdot \mathbf{r}_2} | \lambda'' \rangle \langle \lambda'' | e^{i\mathbf{q}_1 \cdot \mathbf{r}_1} | \lambda' \rangle. \quad (51)$$

Each of the factors  $\langle \lambda | e^{i\mathbf{q}_1 \cdot \mathbf{r}_1} | \lambda' \rangle$  is the sum of the intraband and interband contributions at  $\mathbf{q} \rightarrow \mathbf{0}$ , Eq. (16). Expanding the product (51) we obtain a total of eight summands:

1. One term containing the product of three intraband contributions; we will label it as (3/0) term (three intra- and no inter-band factors). This term is purely classical; the corresponding contribution to the current can be obtained by solving the classical (Boltzmann) kinetic equation.
2. Three terms containing the product of two intraband and one interband contributions; we will label them as (2/1) term (two intra- and one inter-band factors).
3. Three terms containing the product of one intraband and two interband contributions; they will be labeled as (1/2) term.
4. And one term containing the product of three interband contributions; this is a purely quantum contribution; it will be labeled as (0/3) term.

In order to find all these contributions we have to calculate the sums over  $\lambda = (\sigma l \mathbf{k})$ ,  $\lambda' = (\sigma' l' \mathbf{k}')$ ,  $\lambda'' = (\sigma'' l'' \mathbf{k}'')$ , and  $\lambda''' = (\sigma''' l''' \mathbf{k'''})$  in the expression for the current. The summation over the spin indexes  $\sigma$  can be performed easily since each of the matrix elements is proportional to the Kronecker symbol  $\delta_{\sigma\sigma'}$ . The  $l$ -indexes assume two values,  $l = 1, 2$ , so that taking the sums over  $l'$ ,  $l''$  and  $l'''$  is although cumbersome but feasible. The summation over  $\mathbf{k}'$ ,  $\mathbf{k}''$  and  $\mathbf{k'''}$  is quite complicated although the presence of the Kronecker factors  $\delta_{\mathbf{k}, \mathbf{k}' + \mathbf{q}}$  and  $\delta_{\mathbf{k}, \mathbf{k}'} \delta_{\mathbf{k}, \mathbf{k}''}$  in (16) somewhat simplifies the problem. All calculations have to be done at a finite  $\mathbf{q}$  with the limit  $\mathbf{q} \rightarrow \mathbf{0}$  taken at the final stage. Performing this work we obtain the following expression for the third-order current:

$$\underbrace{j_{\alpha}^{(3)}(t)}_{(3/0)} = \underbrace{j_{\alpha}^{(3)}(t)}_{(2/1)} + \underbrace{j_{\alpha}^{(3)}(t)}_{(1/2)} + \underbrace{j_{\alpha}^{(3)}(t)}_{(0/3)}, \quad (52)$$

where

$$\begin{aligned} \underbrace{j_{\alpha}^{(3)}(t)}_{(3/0)} &= \int_{-\infty}^{\infty} d\omega_1 \int_{-\infty}^{\infty} d\omega_2 \int_{-\infty}^{\infty} d\omega_3 E_{\omega_1}^{\beta} E_{\omega_2}^{\gamma} E_{\omega_3}^{\delta} e^{-i(\omega_1 + \omega_2 + \omega_3)t} \\ &\times \frac{1}{(\omega_1 + i\gamma)(\omega_2 + i\gamma)(\omega_3 + i\gamma)} \frac{ie^4 g_s}{6\hbar^3 S} \sum_{l\mathbf{k}} \langle l\mathbf{k} | \hat{v}_{\alpha} | l\mathbf{k} \rangle \frac{\partial^3 f_{l\mathbf{k}}}{\partial k_{\beta} \partial k_{\gamma} \partial k_{\delta}}, \end{aligned} \quad (53)$$

$$\begin{aligned} \underbrace{j_{\alpha}^{(3)}(t)}_{(2/1)} &= \int_{-\infty}^{\infty} d\omega_1 \int_{-\infty}^{\infty} d\omega_2 \int_{-\infty}^{\infty} d\omega_3 E_{\omega_1}^{\beta} E_{\omega_2}^{\gamma} E_{\omega_3}^{\delta} e^{-i(\omega_1 + \omega_2 + \omega_3)t} \\ &\times \frac{1}{(\omega_1 + i\gamma)(\omega_2 + i\gamma)} \frac{ie^4 g_s}{4\hbar^2 S} \sum_{l\mathbf{k}} \frac{\langle \bar{l}\mathbf{k} | \hat{v}_{\alpha} | l\mathbf{k} \rangle}{E_{\bar{l}\mathbf{k}} - E_{l\mathbf{k}} + \hbar\omega_3 + i\hbar\gamma} \eta_{\mathbf{k}}^{\delta} \frac{\partial^2 (f_{l\mathbf{k}} - f_{\bar{l}\mathbf{k}})}{\partial k_{\beta} \partial k_{\gamma}}, \end{aligned} \quad (54)$$

$$\begin{aligned} \underbrace{j_{\alpha}^{(3)}(t)}_{(1/2)} &= \int_{-\infty}^{\infty} d\omega_1 \int_{-\infty}^{\infty} d\omega_2 \int_{-\infty}^{\infty} d\omega_3 E_{\omega_1}^{\beta} E_{\omega_2}^{\gamma} E_{\omega_3}^{\delta} e^{-i(\omega_1 + \omega_2 + \omega_3)t} \\ &\times \frac{1}{\omega_1 + i\gamma} \frac{ie^4 g_s}{4\hbar S} \sum_{l\mathbf{k}} \frac{\langle l\mathbf{k} | \hat{v}_{\alpha} | l\mathbf{k} \rangle}{(E_{l\mathbf{k}} - E_{\bar{l}\mathbf{k}} + \hbar\omega_2 + i\hbar\gamma)(E_{\bar{l}\mathbf{k}} - E_{l\mathbf{k}} + \hbar\omega_3 + i\hbar\gamma)} \eta_{\mathbf{k}}^{\gamma} \eta_{\mathbf{k}}^{\delta} \frac{\partial (f_{l\mathbf{k}} - f_{\bar{l}\mathbf{k}})}{\partial k_{\beta}}, \end{aligned} \quad (55)$$

and

$$\underbrace{j_\alpha^{(3)}(t)}_{(0/3)} = \int_{-\infty}^{\infty} d\omega_1 \int_{-\infty}^{\infty} d\omega_2 \int_{-\infty}^{\infty} d\omega_3 E_{\omega_1}^\beta E_{\omega_2}^\gamma E_{\omega_3}^\delta e^{-i(\omega_1+\omega_2+\omega_3)t} \times \frac{ie^4 g_s}{4S} \sum_{l\mathbf{k}} \frac{\langle \bar{l}\mathbf{k} | \hat{v}_\alpha | l\mathbf{k} \rangle \eta_{l\mathbf{k}}^\beta \eta_{l\mathbf{k}}^\gamma \eta_{l\mathbf{k}}^\delta (f_{l\mathbf{k}} - f_{\bar{l}\mathbf{k}})}{(E_{\bar{l}\mathbf{k}} - E_{l\mathbf{k}} + \hbar\omega_1 + i\hbar\gamma)(E_{l\mathbf{k}} - E_{\bar{l}\mathbf{k}} + \hbar\omega_2 + i\hbar\gamma)(E_{\bar{l}\mathbf{k}} - E_{l\mathbf{k}} + \hbar(\omega_1 + \omega_2 + \omega_3) + i\hbar 3\gamma)}. \quad (56)$$

Notice that, while Eq. (53) has an explicitly symmetric form (with respect to the simultaneous permutations of the frequencies  $\omega_1, \omega_2, \omega_3$  and the indexes  $\beta, \gamma, \delta$ ), the other formulas, Eqs. (54)–(56), do not. They can, however, be always symmetrized by the corresponding permutations ( $(\beta, \omega_1) \leftrightarrow (\gamma, \omega_2)$ , etc.) since the formulas (53)–(56) contain integrals over  $d\omega_1, d\omega_2$  and  $d\omega_3$ . Due to this fact, the expressions for the current  $j_\alpha^{(3)}(t)$  can be written in many different forms. In order to get unambiguous expressions for the current contributions (53)–(56), one should rewrite them in the explicitly symmetric form using the mentioned permutations. We will return to this issue later when the results for the conductivity will be discussed, Section IV B.

Let us further analyze the results presented in Eqs. (53) – (56). One sees a certain structure in these formulas:

1. Each of the contributions (53) – (56) contains three frequency-dependent denominators. In the  $(m/n)$  contribution there are  $m$  denominator factors of the form  $(\omega + i\gamma)$ , so that the corresponding factors have a maximum at  $\omega = 0$  and decrease with the frequency at  $\omega \rightarrow \infty$ , and  $n$  factors of the type  $(\omega + i\gamma + \Delta E)$  having a resonant maximum at the energy of inter-band transitions.
2. The  $(m/n)$ -contribution contains the  $m$ -th derivative of the distribution function. At low temperatures,  $T \ll |\mu| = E_F$ , the integrals over  $d\mathbf{k}$  in all terms except the last one will therefore contain the delta functions  $\delta(k - k_F)$  and its derivatives; here  $k_F = E_F/\hbar v_F$  is the Fermi wave-vector. The corresponding interband contributions will therefore contain resonances at  $\hbar\omega \simeq 2E_F$ . The very last (0/3) contribution does not contain the derivative of the distribution function, therefore it will have a logarithmic feature in its frequency dependence (compare to the interband linear conductivity (47)).
3. The (2/1) and (1/2) contributions have resonances at  $\hbar\omega \simeq 2E_F$  which physically corresponds to the vertical inter-band single-photon transition at the absorption edge. The last, (0/3), contribution has, in addition, a resonant feature at  $\hbar(\omega_1 + \omega_2 + \omega_3) \simeq 2E_F$ , which physically corresponds to the triple-photon transition. Notice that no resonant feature exists at the double-photon transition: there are no terms of the type  $(E_{\bar{l}\mathbf{k}} - E_{l\mathbf{k}} + \hbar(\omega_1 + \omega_2) + i\hbar 2\gamma)$  in the denominators in (53) – (56).
4. The  $(m/n)$  contribution contains  $n$  factors  $\eta_{\mathbf{k}}$ .
5. The  $(m/n)$  contributions with odd  $m$  (i.e., (3/0) and (1/2)) contain only the diagonal (intraband) matrix elements of the velocity  $\langle l\mathbf{k} | \hat{v}_\alpha | l\mathbf{k} \rangle$ . The terms with odd  $n$  (i.e., (2/1) and (0/3)) contain only the off-diagonal (interband) matrix elements of the velocity  $\langle \bar{l}\mathbf{k} | \hat{v}_\alpha | l\mathbf{k} \rangle$ .

As we have mentioned above, taking a proper combination of all possible permutations  $(\omega_1, \beta) \leftrightarrow (\omega_2, \gamma) \leftrightarrow (\omega_3, \delta)$  one can present the formulas (54) – (56) in a totally symmetric form. On the other hand, using certain permutations one can transform the above formulas to a simpler form which facilitates the calculation of the remaining integral. For example, in Appendix B we show how to reduce Eqs. (55) and (56) to simpler forms which contain only one  $\Delta E$ -dependent energy denominators:

$$\underbrace{j_\alpha^{(3)}(t)}_{(1/2)} = \int_{-\infty}^{\infty} d\omega_1 \int_{-\infty}^{\infty} d\omega_2 \int_{-\infty}^{\infty} d\omega_3 E_{\omega_1}^\beta E_{\omega_2}^\gamma E_{\omega_3}^\delta e^{-i(\omega_1+\omega_2+\omega_3)t} \times \frac{1}{\omega_1 + i\gamma} \frac{1}{\omega_2 + \omega_3 + i2\gamma} \frac{ie^4 g_s}{2\hbar^2 S} \sum_{l\mathbf{k}} \frac{\langle l\mathbf{k} | \hat{v}_\alpha | l\mathbf{k} \rangle \eta_{l\mathbf{k}}^\gamma \eta_{l\mathbf{k}}^\delta}{E_{\bar{l}\mathbf{k}} - E_{l\mathbf{k}} + \hbar\omega_2 + i\hbar\gamma} \frac{\partial(f_{l\mathbf{k}} - f_{\bar{l}\mathbf{k}})}{\partial k_\beta}, \quad (57)$$

$$\underbrace{j_\alpha^{(3)}(t)}_{(0/3)} = \int_{-\infty}^{\infty} d\omega_1 \int_{-\infty}^{\infty} d\omega_2 \int_{-\infty}^{\infty} d\omega_3 E_{\omega_1}^\beta E_{\omega_2}^\gamma E_{\omega_3}^\delta e^{-i(\omega_1+\omega_2+\omega_3)t} \times \frac{(\omega_1 + \omega_2 + \omega_3 + i3\gamma)\mathcal{F}(\omega_1 + i\gamma) - (\omega_1 + i\gamma)\mathcal{F}(\omega_1 + \omega_2 + \omega_3 + i3\gamma)}{(\omega_1 + \omega_2 + i2\gamma)(2\omega_1 + \omega_2 + \omega_3 + i4\gamma)(\omega_2 + \omega_3 + i2\gamma)} \quad (58)$$

where

$$\mathcal{F}(\omega + i\gamma) = \frac{ie^4 g_s}{2\hbar^2 S} \sum_{l\mathbf{k}} \frac{\langle \bar{l}\mathbf{k} | \hat{v}_\alpha | l\mathbf{k} \rangle \eta_\mathbf{k}^\beta \eta_\mathbf{k}^\gamma \eta_\mathbf{k}^\delta (f_{l\mathbf{k}} - f_{\bar{l}\mathbf{k}})}{E_{\bar{l}\mathbf{k}} - E_{l\mathbf{k}} + \hbar(\omega + i\gamma)}. \quad (59)$$

The formulas (57) and (58) are equivalent to Eqs. (55) and (56), respectively. For calculations below we will use the latter forms, Eqs. (57) and (58).

Equations (53) – (58) contain one remaining integration (the sums  $\sum_{\mathbf{k}}$ ). In the next section we define the third-order conductivity and explicitly calculate them.

## B. Third-order conductivity

We define the third-order conductivity tensor of graphene  $\sigma_{\alpha\beta\gamma\delta}^{(3)}(\omega_1, \omega_2, \omega_3)$  as follows

$$j_\alpha^{(3)}(t) = \int_{-\infty}^{\infty} d\omega_1 \int_{-\infty}^{\infty} d\omega_2 \int_{-\infty}^{\infty} d\omega_3 \sigma_{\alpha\beta\gamma\delta}^{(3)}(\omega_1, \omega_2, \omega_3) E_{\omega_1}^\beta E_{\omega_2}^\gamma E_{\omega_3}^\delta e^{-i(\omega_1 + \omega_2 + \omega_3)t}. \quad (60)$$

In accordance with (53) – (56) it contains four contributions which we calculate now.

### 1. (3/0) contribution

The (3/0) contribution to the third-order conductivity assumes the form

$$\underbrace{\sigma_{\alpha\beta\gamma\delta}^{(3)}(\omega_1, \omega_2, \omega_3)}_{(3/0)} = \frac{W_{\alpha\beta\gamma\delta}^{(3/0)}}{(\omega_1 + i\gamma)(\omega_2 + i\gamma)(\omega_3 + i\gamma)}, \quad (61)$$

where the factor  $W_{\alpha\beta\gamma\delta}^{(3/0)}$  is

$$W_{\alpha\beta\gamma\delta}^{(3/0)} = \frac{ie^4 g_s}{6\hbar^3 S} \sum_{l\mathbf{k}} \langle l\mathbf{k} | \hat{v}_\alpha | l\mathbf{k} \rangle \frac{\partial^3 f_{l\mathbf{k}}}{\partial k_\beta \partial k_\gamma \partial k_\delta}. \quad (62)$$

Substituting in (62) the matrix element of the velocity (24) and integrating by part we rewrite the function  $W_{\alpha\beta\gamma\delta}^{(3/0)}$  in the form

$$W_{\alpha\beta\gamma\delta}^{(3/0)} = \frac{ie^4 g_s}{6\hbar^4 S} \sum_{l\mathbf{k}} \frac{\partial f(E_{l\mathbf{k}})}{\partial E} \frac{\partial^3 E_{l\mathbf{k}}}{\partial k_\alpha \partial k_\beta \partial k_\gamma} \frac{\partial E_{l\mathbf{k}}}{\partial k_\delta} \quad (63)$$

Due to the factor  $\partial f(E_{l\mathbf{k}})/\partial E$  only the vicinity of the Fermi level contributes to the integral. Therefore the integration over the whole Brillouin zone in (63) is reduced to the integration over the vicinity of two Dirac points. The both Dirac points contribute equally to the integral which leads to an additional, valley degeneracy factor  $g_v = 2$ . Near the Dirac points we have  $E_{l\mathbf{k}} = (-1)^l \hbar v_F k$ , Eq. (13). The differentiation gives

$$\frac{\partial E_{l\mathbf{k}}}{\partial k_\delta} = (-1)^l \hbar v_F \frac{k_\delta}{k}, \quad (64)$$

$$\frac{\partial^3 E_{l\mathbf{k}}}{\partial k_\alpha \partial k_\beta \partial k_\gamma} = (-1)^l \hbar v_F \left( -\frac{k_\alpha \delta_{\beta\gamma} + k_\beta \delta_{\alpha\gamma} + k_\gamma \delta_{\alpha\beta}}{k^3} + 3 \frac{k_\alpha k_\beta k_\gamma}{k^5} \right). \quad (65)$$

Substituting (64) and (65) back to Eq. (63) and calculating the integral leads to the following result (at  $T \ll |\mu|$ ):

$$W_{\alpha\beta\gamma\delta}^{(3/0)} = \frac{ie^4 g_s g_v v_F}{96\pi\hbar^3 k_F} \left( \delta_{\alpha\beta} \delta_{\gamma\delta} + \delta_{\alpha\gamma} \delta_{\beta\delta} + \delta_{\alpha\delta} \delta_{\beta\gamma} \right). \quad (66)$$

Here the angular integration in the  $\mathbf{k}$ -space [ $\mathbf{k} = k(\cos \phi, \sin \phi)$ ] has been performed using Eqs. (A5) and (A6).

Thus, the (3/0) contribution to the third-order conductivity is

$$\underbrace{\sigma_{\alpha\beta\gamma\delta}^{(3)}(\omega_1, \omega_2, \omega_3)}_{(3/0)} = \sigma_0^{(3)} \mathcal{S}_{\alpha\beta\gamma\delta}^{(3/0)}(\Omega_1, \Omega_2, \Omega_3), \quad (67)$$

where

$$\sigma_0^{(3)} = \frac{e^4 g_s g_v \hbar v_F^2}{16\pi E_F^4} \quad (68)$$

and

$$\mathcal{S}_{\alpha\beta\gamma\delta}^{(3/0)}(\Omega_1, \Omega_2, \Omega_3) = \frac{i}{6} \frac{\delta_{\alpha\beta}\delta_{\gamma\delta} + \delta_{\alpha\gamma}\delta_{\beta\delta} + \delta_{\alpha\delta}\delta_{\beta\gamma}}{(\Omega_1 + i\Gamma)(\Omega_2 + i\Gamma)(\Omega_3 + i\Gamma)}. \quad (69)$$

The contribution (69) has an explicitly symmetric form.

## 2. (2/1) contribution

The (2/1) contribution to the third-order conductivity assumes the form

$$\underbrace{\sigma_{\alpha\beta\gamma\delta}^{(3)}(\omega_1, \omega_2, \omega_3)}_{(2/1)} = \frac{W_{\alpha\beta\gamma\delta}^{(2/1)}(\omega_3 + i\gamma)}{(\omega_1 + i\gamma)(\omega_2 + i\gamma)}, \quad (70)$$

where the function  $W_{\alpha\beta\gamma\delta}^{(2/1)}(\omega + i\gamma)$  is

$$W_{\alpha\beta\gamma\delta}^{(2/1)}(\omega + i\gamma) = \frac{ie^4 g_s}{4\hbar^3 S} \sum_{l\mathbf{k}} \frac{\langle \bar{l}\mathbf{k} | \hat{v}_\alpha | l\mathbf{k} \rangle}{E_{\bar{l}\mathbf{k}} - E_{l\mathbf{k}} + \hbar(\omega + i\gamma)} \eta_\mathbf{k}^\delta \frac{\partial^2(f_{l\mathbf{k}} - f_{\bar{l}\mathbf{k}})}{\partial k_\beta \partial k_\gamma}, \quad (71)$$

Substituting in (71) the off-diagonal matrix element of the velocity (25), integrating by part and designating  $E_{2\mathbf{k}} = -E_{1\mathbf{k}} \equiv E_\mathbf{k} \geq 0$  we rewrite the function  $W_{\alpha\beta\gamma\delta}^{(2/1)}$  in the form

$$W_{\alpha\beta\gamma\delta}^{(2/1)}(\omega + i\gamma) = -\frac{ie^4 g_s}{8\hbar^3 S} \sum_{\mathbf{k}} \frac{\partial}{\partial k_\gamma} \left[ \left( \frac{2E_\mathbf{k}}{2E_\mathbf{k} + \hbar(\omega + i\gamma)} - \frac{2E_\mathbf{k}}{2E_\mathbf{k} - \hbar(\omega + i\gamma)} \right) \eta_\mathbf{k}^\alpha \eta_\mathbf{k}^\delta \right] \frac{\partial(f_{1\mathbf{k}} - f_{2\mathbf{k}})}{\partial k_\beta}. \quad (72)$$

At low temperatures,  $T \ll |\mu|$ , the distribution function difference in (72) is  $f_{1\mathbf{k}} - f_{2\mathbf{k}} \approx \Theta(k - k_F)$  for both signs of the chemical potential. Then the integrand in (72) is proportional to  $\delta(k - k_F)$ . Due to this delta function the integration over the whole Brillouin zone is reduced to the one over the vicinity of the Dirac points. Integrating (72) over  $dk$  with the help of the delta-function and over  $d\phi$  using formulas (A5) and (A6) we obtain:

$$\begin{aligned} W_{\alpha\beta\gamma\delta}^{(2/1)}(\omega + i\gamma) &= \frac{-ie^4 g_s g_v}{32\pi \hbar^3 k_F^2} \left\{ \delta_{\alpha\delta}\delta_{\beta\gamma} \left( \frac{1}{[1 + (\Omega + i\Gamma)/2]^2} - \frac{1}{[1 - (\Omega + i\Gamma)/2]^2} \right) \right. \\ &\quad \left. + \frac{1}{4} \left( \delta_{\alpha\beta}\delta_{\gamma\delta} + \delta_{\alpha\gamma}\delta_{\beta\delta} + \delta_{\alpha\delta}\delta_{\beta\gamma} \right) \left( \frac{(\Omega + i\Gamma)/2}{[1 + (\Omega + i\Gamma)/2]^2} + \frac{(\Omega + i\Gamma)/2}{[1 - (\Omega + i\Gamma)/2]^2} \right) \right\}. \end{aligned} \quad (73)$$

The (2/1) conductivity is then

$$\underbrace{\tilde{\sigma}_{\alpha\beta\gamma\delta}^{(3)}(\omega_1, \omega_2, \omega_3)}_{(2/1)} = \sigma_0^{(3)} \tilde{\mathcal{S}}_{\alpha\beta\gamma\delta}^{(2/1)}(\Omega_1, \Omega_2, \Omega_3), \quad (74)$$

where

$$\begin{aligned} \tilde{\mathcal{S}}_{\alpha\beta\gamma\delta}^{(2/1)}(\Omega_1, \Omega_2, \Omega_3) &= \frac{i}{2(\Omega_1 + i\Gamma)(\Omega_2 + i\Gamma)} \left\{ \delta_{\alpha\delta}\delta_{\beta\gamma} \left( \frac{1}{[1 - (\Omega_3 + i\Gamma)/2]^2} - \frac{1}{[1 + (\Omega_3 + i\Gamma)/2]^2} \right) \right. \\ &\quad \left. - \frac{1}{4} \left( \delta_{\alpha\beta}\delta_{\gamma\delta} + \delta_{\alpha\gamma}\delta_{\beta\delta} + \delta_{\alpha\delta}\delta_{\beta\gamma} \right) \left( \frac{(\Omega_3 + i\Gamma)/2}{[1 + (\Omega_3 + i\Gamma)/2]^2} + \frac{(\Omega_3 + i\Gamma)/2}{[1 - (\Omega_3 + i\Gamma)/2]^2} \right) \right\}, \end{aligned} \quad (75)$$

and we have placed tilde over  $\tilde{\sigma}$  and  $\tilde{S}$  in order to emphasize that this form of the result is not symmetric. If to substitute Eqs. (74) – (75) in the expression (60) one would get a correct result for the corresponding current contribution, since Eq. (60) contains the integration over all three omega's. In order to use the formulas (74) – (75) independently of (60), they still should be symmetrized (see Eq. (95) below).

### 3. (1/2) contribution

To calculate the (1/2) contribution to the third-order conductivity we use the form (57), so that

$$\underbrace{\sigma_{\alpha\beta\gamma\delta}^{(3)}(\omega_1, \omega_2, \omega_3)}_{(1/2)} = \frac{W_{\alpha\beta\gamma\delta}^{(1/2)}(\omega_2 + i\gamma)}{(\omega_1 + i\gamma)(\omega_2 + \omega_3 + i2\gamma)}, \quad (76)$$

where

$$W_{\alpha\beta\gamma\delta}^{(1/2)}(\omega + i\gamma) = \frac{ie^4 g_s}{2\hbar^2 S} \sum_{l\mathbf{k}} \frac{\langle l\mathbf{k} | \hat{v}_\alpha | l\mathbf{k} \rangle}{E_{l\mathbf{k}} - E_{l\mathbf{k}} + \hbar(\omega + i\gamma)} \eta_\mathbf{k}^\gamma \eta_\mathbf{k}^\delta \frac{\partial(f_{l\mathbf{k}} - f_{\bar{l}\mathbf{k}})}{\partial k_\beta}. \quad (77)$$

The calculation of the factor  $W_{\alpha\beta\gamma\delta}^{(1/2)}(\omega + i\gamma)$  is similar. We use the diagonal matrix element of the velocity (24) and the presence of the delta-function in the integrand. Performing the integration and using the formulas (A5) and (A6) we obtain

$$W_{\alpha\beta\gamma\delta}^{(1/2)}(\omega + i\gamma) = \frac{ie^4 g_s g_v \hbar v_F^2}{64\pi \hbar^2 E_F^2} (4\delta_{\alpha\beta}\delta_{\gamma\delta} - (\delta_{\alpha\beta}\delta_{\gamma\delta} + \delta_{\alpha\gamma}\delta_{\beta\delta} + \delta_{\alpha\delta}\delta_{\gamma\beta})) \left( \frac{1}{1 + (\Omega + i\Gamma)/2} - \frac{1}{1 - (\Omega + i\Gamma)/2} \right). \quad (78)$$

The (non-symmetrized) (1/2) conductivity is then

$$\underbrace{\tilde{\sigma}_{\alpha\beta\gamma\delta}^{(3)}(\omega_1, \omega_2, \omega_3)}_{(1/2)} = \sigma_0^{(3)} \tilde{S}_{\alpha\beta\gamma\delta}^{(1/2)}(\Omega_1, \Omega_2, \Omega_3), \quad (79)$$

where

$$\tilde{S}_{\alpha\beta\gamma\delta}^{(1/2)}(\Omega_1, \Omega_2, \Omega_3) = \frac{i[4\delta_{\alpha\beta}\delta_{\gamma\delta} - (\delta_{\alpha\beta}\delta_{\gamma\delta} + \delta_{\alpha\gamma}\delta_{\beta\delta} + \delta_{\alpha\delta}\delta_{\gamma\beta})]}{4(\Omega_1 + i\Gamma)(\Omega_2 + \Omega_3 + i2\Gamma)} \left( \frac{1}{1 + (\Omega_2 + i\Gamma)/2} - \frac{1}{1 - (\Omega_2 + i\Gamma)/2} \right). \quad (80)$$

### 4. (0/3) contribution

To calculate the (0/3) contribution to the third-order conductivity we use the form (58), so that

$$\underbrace{\sigma_{\alpha\beta\gamma\delta}^{(3)}(\omega_1, \omega_2, \omega_3)}_{(0/3)} = \frac{(\omega_1 + \omega_2 + \omega_3 + i3\gamma)\mathcal{F}(\omega_1 + i\gamma) - (\omega_1 + i\gamma)\mathcal{F}(\omega_1 + \omega_2 + \omega_3 + i3\gamma)}{(\omega_1 + \omega_2 + i2\gamma)(2\omega_1 + \omega_2 + \omega_3 + i4\gamma)(\omega_2 + \omega_3 + i2\gamma)}. \quad (81)$$

Now we calculate the function  $\mathcal{F}$  defined in Eq. (59). Substituting the matrix element of the velocity (25) and using that  $E_{\bar{l}\mathbf{k}} = -E_{l\mathbf{k}}$  we get

$$\mathcal{F}(\omega + i\gamma) = \frac{ie^4 g_s}{4\hbar^3 S} \sum_{l\mathbf{k}} \frac{-2E_{l\mathbf{k}}}{-2E_{l\mathbf{k}} + \hbar(\omega + i\gamma)} \eta_\mathbf{k}^\alpha \eta_\mathbf{k}^\beta \eta_\mathbf{k}^\gamma \eta_\mathbf{k}^\delta (f_{l\mathbf{k}} - f_{\bar{l}\mathbf{k}}). \quad (82)$$

Taking the sum over  $l = 1, 2$  and defining the (positive) energy  $E_\mathbf{k} \equiv E_{2\mathbf{k}} = -E_{1\mathbf{k}} \geq 0$  we reduce the expression for  $\mathcal{F}(\omega + i\gamma)$  to the form

$$\mathcal{F}(\omega + i\gamma) = \frac{ie^4 g_s}{4\hbar^3 S} \sum_{\mathbf{k}} \eta_\mathbf{k}^\alpha \eta_\mathbf{k}^\beta \eta_\mathbf{k}^\gamma \eta_\mathbf{k}^\delta \left( \frac{2E_\mathbf{k}}{2E_\mathbf{k} + \hbar(\omega + i\gamma)} - \frac{2E_\mathbf{k}}{2E_\mathbf{k} - \hbar(\omega + i\gamma)} \right) (f_{1\mathbf{k}} - f_{2\mathbf{k}}). \quad (83)$$

The Fermi functions difference  $(f_{1\mathbf{k}} - f_{2\mathbf{k}})$  is proportional to the Heaviside function  $\Theta(k - k_F)$  at zero temperature, so that the integration in (83) is performed over the Brillouin zone excluding the small vicinity  $k < k_F$  of the Dirac

points. Since the functions  $\eta_{\mathbf{k}}$  are proportional to  $1/k$ , Eq. (18), the integrals in (83) quickly converge when  $k$  moves away from the Dirac points, so that we can use the near-Dirac-points expansions (13) – (14) and extend the integration up to  $k = \pm\infty$ ,

$$\mathcal{F}(\omega + i\gamma) = \frac{ie^4 g_s g_v}{4\hbar^3 (2\pi)^2} \int_0^{2\pi} d\phi \int_0^\infty \frac{dk}{k^7} \epsilon_{\alpha\mu} k_\mu \epsilon_{\beta\nu} k_\nu \epsilon_{\gamma\sigma} k_\sigma \epsilon_{\delta\rho} k_\rho \left( \frac{k}{k + \frac{\omega+i\gamma}{2v_F}} - \frac{k}{k - \frac{\omega+i\gamma}{2v_F}} \right) \Theta(k - k_F). \quad (84)$$

Integrating over  $d\phi$  with the help of Eq. (A6) and using the identity (A4) we finally get

$$\mathcal{F}(\omega + i\gamma) = \frac{ie^4 g_s g_v}{16\pi \hbar^3 k_F^2} \left( \delta_{\alpha\beta} \delta_{\gamma\delta} + \delta_{\alpha\gamma} \delta_{\beta\delta} + \delta_{\alpha\delta} \delta_{\beta\gamma} \right) \mathcal{K}(\Omega + i\Gamma), \quad (85)$$

where

$$\mathcal{K}(\Omega + i\Gamma) = -\frac{1}{4} \left( \int_1^\infty + \int_{-\infty}^{-1} \right) \frac{dx}{x^2} \frac{1}{x - \frac{\Omega+i\Gamma}{2}} = \frac{1}{(\Omega + i\Gamma)^2} \left( \ln \frac{2 - (\Omega + i\Gamma)}{2 + (\Omega + i\Gamma)} + (\Omega + i\Gamma) \right). \quad (86)$$

The (non-symmetrized) contribution (0/3) to the third-order conductivity is then

$$\underbrace{\tilde{\sigma}_{\alpha\beta\gamma\delta}^{(3)}(\omega_1, \omega_2, \omega_3)}_{(0/3)} = \sigma_0^{(3)} \tilde{\mathcal{S}}_{\alpha\beta\gamma\delta}^{(0/3)}(\Omega_1, \Omega_2, \Omega_3), \quad (87)$$

$$\begin{aligned} \tilde{\mathcal{S}}_{\alpha\beta\gamma\delta}^{(0/3)}(\Omega_1, \Omega_2, \Omega_3) &= i \left( \delta_{\alpha\beta} \delta_{\gamma\delta} + \delta_{\alpha\gamma} \delta_{\beta\delta} + \delta_{\alpha\delta} \delta_{\beta\gamma} \right) \\ &\times \frac{(\Omega_1 + \Omega_2 + \Omega_3 + i3\Gamma) \mathcal{K}(\Omega_1 + i\Gamma) - (\Omega_1 + i\Gamma) \mathcal{K}(\Omega_1 + \Omega_2 + \Omega_3 + i3\Gamma)}{(\Omega_1 + \Omega_2 + i2\Gamma)(2\Omega_1 + \Omega_2 + \Omega_3 + i4\Gamma)(\Omega_2 + \Omega_3 + i2\Gamma)}. \end{aligned} \quad (88)$$

### C. Summary of the third-order conductivity contributions

The analytical expression for the third-order conductivity thus assumes the form

$$\sigma_{\alpha\beta\gamma\delta}^{(3)}(\omega_1, \omega_2, \omega_3) = \sigma_0^{(3)} \mathcal{S}_{\alpha\beta\gamma\delta}^{(3)}(\Omega_1, \Omega_2, \Omega_3) \quad (89)$$

(compare with (43)), where  $\sigma_0^{(3)}$  is defined in (68) and the dimensionless function

$$\mathcal{S}_{\alpha\beta\gamma\delta}^{(3)}(\Omega_1, \Omega_2, \Omega_3) = \mathcal{S}_{\alpha\beta\gamma\delta}^{(3/0)}(\Omega_1, \Omega_2, \Omega_3) + \tilde{\mathcal{S}}_{\alpha\beta\gamma\delta}^{(2/1)}(\Omega_1, \Omega_2, \Omega_3) + \tilde{\mathcal{S}}_{\alpha\beta\gamma\delta}^{(1/2)}(\Omega_1, \Omega_2, \Omega_3) + \tilde{\mathcal{S}}_{\alpha\beta\gamma\delta}^{(0/3)}(\Omega_1, \Omega_2, \Omega_3) \quad (90)$$

consists of four contributions,

$$\mathcal{S}_{\alpha\beta\gamma\delta}^{(3/0)}(\Omega_1, \Omega_2, \Omega_3) = i \frac{\delta_{\alpha\beta} \delta_{\gamma\delta} + \delta_{\alpha\gamma} \delta_{\beta\delta} + \delta_{\alpha\delta} \delta_{\beta\gamma}}{6(\Omega_1 + i\Gamma)(\Omega_2 + i\Gamma)(\Omega_3 + i\Gamma)}, \quad (91)$$

$$\begin{aligned} \tilde{\mathcal{S}}_{\alpha\beta\gamma\delta}^{(2/1)}(\Omega_1, \Omega_2, \Omega_3) &= \frac{i}{2(\Omega_1 + i\Gamma)(\Omega_2 + i\Gamma)} \left\{ \delta_{\alpha\delta} \delta_{\beta\gamma} \left( \frac{1}{[1 - (\Omega_3 + i\Gamma)/2]^2} - \frac{1}{[1 + (\Omega_3 + i\Gamma)/2]^2} \right) \right. \\ &\quad \left. - \frac{\delta_{\alpha\beta} \delta_{\gamma\delta} + \delta_{\alpha\gamma} \delta_{\beta\delta} + \delta_{\alpha\delta} \delta_{\beta\gamma}}{4} \left( \frac{(\Omega_3 + i\Gamma)/2}{[1 + (\Omega_3 + i\Gamma)/2]^2} + \frac{(\Omega_3 + i\Gamma)/2}{[1 - (\Omega_3 + i\Gamma)/2]^2} \right) \right\}, \end{aligned} \quad (92)$$

$$\begin{aligned} \tilde{\mathcal{S}}_{\alpha\beta\gamma\delta}^{(1/2)}(\Omega_1, \Omega_2, \Omega_3) &= \frac{i}{(\Omega_1 + i\Gamma)(\Omega_2 + \Omega_3 + i2\Gamma)} \left( \frac{1}{1 + (\Omega_2 + i\Gamma)/2} - \frac{1}{1 - (\Omega_2 + i\Gamma)/2} \right) \\ &\times \left( \delta_{\alpha\beta} \delta_{\gamma\delta} - \frac{\delta_{\alpha\beta} \delta_{\gamma\delta} + \delta_{\alpha\gamma} \delta_{\beta\delta} + \delta_{\alpha\delta} \delta_{\beta\gamma}}{4} \right), \end{aligned} \quad (93)$$

$\alpha\beta\gamma\delta$	$\delta_{\alpha\beta}\delta_{\gamma\delta} + \delta_{\alpha\gamma}\delta_{\beta\delta} + \delta_{\alpha\delta}\delta_{\beta\gamma}$	$\delta_{\alpha\delta}\delta_{\beta\gamma}$	$\delta_{\alpha\beta}\delta_{\gamma\delta}$
$xyxy \& yxyx$	1	0	0
$xyyx \& yxxy$	1	1	0
$xxyy \& yyxx$	1	0	1
$xxxx \& yyyy$	3	1	1

TABLE I: Values of the Kronecker-symbol combinations which enter Eqs. (91) – (94).

and

$$\begin{aligned} \tilde{\mathcal{S}}_{\alpha\beta\gamma\delta}^{(0/3)}(\Omega_1, \Omega_2, \Omega_3) &= i \left( \delta_{\alpha\beta}\delta_{\gamma\delta} + \delta_{\alpha\gamma}\delta_{\beta\delta} + \delta_{\alpha\delta}\delta_{\beta\gamma} \right) \\ &\times \frac{(\Omega_1 + \Omega_2 + \Omega_3 + i3\Gamma)\mathcal{K}(\Omega_1 + i\Gamma) - (\Omega_1 + i\Gamma)\mathcal{K}(\Omega_1 + \Omega_2 + \Omega_3 + i3\Gamma)}{(\Omega_1 + \Omega_2 + i2\Gamma)(2\Omega_1 + \Omega_2 + \Omega_3 + i4\Gamma)(\Omega_2 + \Omega_3 + i2\Gamma)}. \end{aligned} \quad (94)$$

The  $\mathcal{K}(\Omega + i\Gamma)$  function in (94) is defined in (86) and the tildes remind that the corresponding contributions do not have a symmetric form. Each of the non-symmetrized results (92) – (94) can be presented in the symmetric form (without tilde) by permuting the tilde-expressions:

$$\begin{aligned} \sigma_{\alpha\beta\gamma\delta}^{(3)}(\omega_1, \omega_2, \omega_3) &= \frac{1}{3!} \left( \tilde{\sigma}_{\alpha\beta\gamma\delta}^{(3)}(\omega_1, \omega_2, \omega_3) + \tilde{\sigma}_{\alpha\beta\delta\gamma}^{(3)}(\omega_1, \omega_3, \omega_2) + \tilde{\sigma}_{\alpha\gamma\beta\delta}^{(3)}(\omega_2, \omega_1, \omega_3) \right. \\ &\quad \left. + \tilde{\sigma}_{\alpha\gamma\delta\beta}^{(3)}(\omega_2, \omega_3, \omega_1) + \tilde{\sigma}_{\alpha\delta\beta\gamma}^{(3)}(\omega_3, \omega_1, \omega_2) + \tilde{\sigma}_{\alpha\delta\gamma\beta}^{(3)}(\omega_3, \omega_2, \omega_1) \right). \end{aligned} \quad (95)$$

The third-order conductivity (89) satisfies the relation

$$\left[ \sigma_{\alpha\beta\gamma\delta}^{(3)}(-\omega_1, -\omega_2, -\omega_3) \right]^* = \sigma_{\alpha\beta\gamma\delta}^{(3)}(\omega_1, \omega_2, \omega_3). \quad (96)$$

As seen from Table I, there are three independent third-order conductivity components

$$\sigma_{xyxy}^{(3)} = \sigma_{yxyx}^{(3)}, \quad \sigma_{xxyy}^{(3)} = \sigma_{yxxxy}^{(3)}, \quad \sigma_{xxyy}^{(3)} = \sigma_{yyxx}^{(3)}, \quad (97)$$

and the component  $\sigma_{xxxx}^{(3)} = \sigma_{yyyy}^{(3)}$  satisfies the equality

$$\sigma_{xxxx}^{(3)} = \sigma_{xxyy}^{(3)} + \sigma_{xxyy}^{(3)} + \sigma_{xyxy}^{(3)}. \quad (98)$$

This agrees with the phenomenological relations for the third-order response function in an isotropic medium.

The analytical formulas (89) – (95) obtained in this Section present the main results of this work. They describe a very large number of different experimental situations and different physical effects, such as the third harmonic generation, static and dynamic photoconductivity, four-wave mixing, dc current induced second harmonic, as well as sum- and difference-frequency generation, a third-order response to a pulse excitation, etc.. It is impossible to analyze all the consequences of these formulas in one paper. A small part of them is investigated in the subsequent Sections.

## V. LIMITING CASES

In this Section we discuss the obtained results in different limiting cases: at low (radio/microwave/terahertz) and high (infrared/optical) frequencies, as well as near the single-photon and triple-photon absorption resonances.

### A. Microwave/terahertz response of doped graphene, $\hbar\omega \lesssim 2E_F$

First, consider the system response at low frequencies, when all frequency parameters satisfy the conditions  $|\Omega_j + i\Gamma|/2 \ll 1$ , or  $\Omega_j \ll 2$  and  $\Gamma \ll 2$ . The latter one,  $\Gamma/2 = \hbar/2E_F\tau \ll 1$  or  $2v_F\tau\sqrt{\pi n_s} \gg 1$ , means that the mean-free path exceeds the average distance between electrons. This condition is usually fulfilled in experiments (for example,

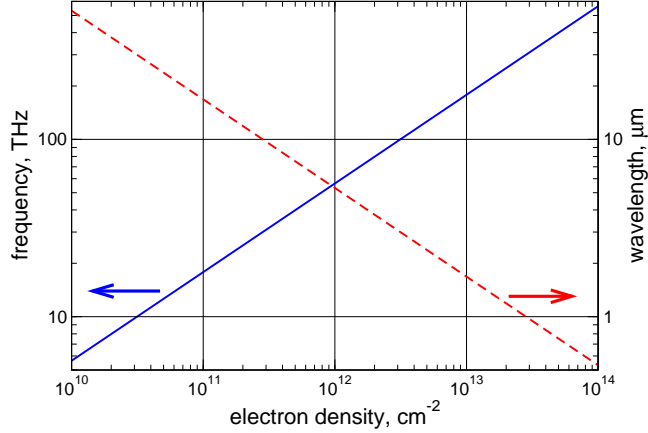


FIG. 3: The relation  $\hbar\omega = 2E_F = 2\hbar v_F \sqrt{\pi n_s}$  plotted as the frequency  $f = \omega/2\pi$  and the wavelength  $\lambda = c/f$  vs the electron density  $n_s$ .

at  $n_s = 10^{12} \text{ cm}^{-2}$  and  $\tau = 0.1 \text{ ps}$  we have  $2v_F\tau\sqrt{\pi n_s} \approx 20\sqrt{\pi} \approx 35$ ). The second condition,  $\hbar\omega \ll 2E_F$ , is satisfied at up to mid-infrared frequencies, see Figure 3. For example, at the density  $n_s = 10^{12} \text{ cm}^{-2}$  this condition corresponds to  $f \lesssim 60 \text{ THz}$ .

As seen from Eqs. (92) and (93), the (2/1) and (1/2) contributions to the third-order conductivity at  $|\Omega_j + i\Gamma|/2 \ll 1$  are of order of  $O(1/\Omega)$ . Expanding the function  $\mathcal{K}(z)$  at  $|z| \ll 1$ ,

$$\mathcal{K}(z) \approx -\frac{z}{12} - \frac{z^3}{80}, \quad |z| \ll 1, \quad (99)$$

we see that the (0/3) contribution (94) to  $\sigma_{\alpha\beta\gamma\delta}(\omega_1, \omega_2, \omega_3)$  is also of order of  $O(1/\Omega)$ . The largest contribution to the third-order conductivity at low frequencies at  $|\Omega_j + i\Gamma|/2 \ll 1$  is thus given by the quasi-classical (3/0) term (91) which has the order  $O(1/\Omega^3)$ :

$$\sigma_{\alpha\beta\gamma\delta}^{(3)}(\omega_1, \omega_2, \omega_3) \approx \underbrace{\sigma_{\alpha\beta\gamma\delta}^{(3)}(\omega_1, \omega_2, \omega_3)}_{(3/0)} = \sigma_0^{(3)} \frac{i}{6} \frac{\delta_{\alpha\beta}\delta_{\gamma\delta} + \delta_{\alpha\gamma}\delta_{\beta\delta} + \delta_{\alpha\delta}\delta_{\beta\gamma}}{(\Omega_1 + i\Gamma)(\Omega_2 + i\Gamma)(\Omega_3 + i\Gamma)}, \quad |\Omega_j + i\Gamma|/2 \ll 1. \quad (100)$$

This result was obtained within the quasi-classical approach in Ref.<sup>19</sup>.

From this point on we will estimate the absolute value of the nonlinear parameters of graphene at different frequencies. Apart from the third conductivity  $\sigma^{(3)}$  we will also estimate the third susceptibility  $\chi^{(3)} \simeq \sigma^{(3)}/\omega d_{gr}$  which is more commonly used in the nonlinear-optics literature. Here  $d_{gr} \approx 3.3 \times 10^{-8} \text{ cm}$  is the effective thickness of a single graphene layer which is usually used to compare the nonlinear properties of two-dimensional graphene with those of three-dimensional nonlinear crystals.

Consider the practically important frequency range of about 1 THz. Assuming that all frequencies are the same, we get for  $|\sigma_{xxxx}^{(3)}(\omega, \omega, \omega)|$ :

$$|\sigma_{xxxx}^{(3)}(\omega, \omega, \omega)| \simeq \frac{e^4 v_F^2}{8\pi\hbar^2 E_F} \frac{1}{|\omega + i\gamma|^3}. \quad (101)$$

If  $f = \omega/2\pi \simeq 1 \text{ THz}$ , the effective scattering time  $\tau = 1/\gamma \simeq 1 \text{ ps}$ , and the electron density  $n_s = 10^{12} \text{ cm}^{-2}$  we get

$$|\sigma_{xxxx}^{(3)}(\omega, \omega, \omega)| \simeq 4 \times 10^5 \text{ esu} \text{ and } |\chi_{xxxx}^{(3)}(\omega, \omega, \omega)| \simeq 1.9 \text{ esu}, \quad (102)$$

where we have used electrostatic units. Comparing the third-order current  $j^{(3)} \simeq \sigma^{(3)} E^3$  with the first-order one  $j^{(1)} \simeq \sigma^{(1)} E$ , we see that  $j^{(3)}$  becomes equal to  $j^{(1)}$  in electric fields of order of 70 esu or 21 kV/cm at the assumed parameters. The nonlinear effects in graphene at THz frequencies are thus quite essential in the electric field of the kV/cm range. At lower frequencies and densities the electric field required for the observation of the nonlinear effects is even smaller.

### B. Optical response of intrinsic graphene, $\hbar\omega \gg 2E_F$

Now consider the opposite limit  $|\Omega_j + i\Gamma|/2 \gg 1$ . This case was realized in most optical experiments where intrinsic (not intentionally doped) graphene was used. As will be seen below, at large frequencies we have to keep the terms of order  $\Omega^{-3}$  and  $\Omega^{-4}$ .

The (3/0) contribution (91) has the order  $O(1/\Omega^3)$  and should be taken as it is. For the (2/1) term we have at  $|\Omega_j + i\Gamma|/2 \gg 1$ :

$$\underbrace{\sigma_{\alpha\beta\gamma\delta}^{(3)}(\omega_1, \omega_2, \omega_3)}_{(2/1)} \approx \sigma_0^{(3)} \frac{-i}{2} \frac{\delta_{\alpha\beta}\delta_{\gamma\delta} + \delta_{\alpha\gamma}\delta_{\beta\delta} + \delta_{\alpha\delta}\delta_{\beta\gamma}}{(\Omega_1 + i\Gamma)(\Omega_2 + i\Gamma)(\Omega_3 + i\Gamma)}. \quad (103)$$

This result is symmetric, and the correction to (103) is of order  $O(1/\Omega^5)$ . Now consider the (1/2) term. Expanding it at large frequencies we get

$$\tilde{\sigma}_{\alpha\beta\gamma\delta}^{(3)}(\omega_1, \omega_2, \omega_3) \approx i\sigma_0^{(3)} \frac{4}{(\Omega_1 + i\Gamma)(\Omega_2 + \Omega_3 + i2\Gamma)(\Omega_2 + i\Gamma)} \left( \delta_{\alpha\beta}\delta_{\gamma\delta} - \frac{\delta_{\alpha\beta}\delta_{\gamma\delta} + \delta_{\alpha\gamma}\delta_{\beta\delta} + \delta_{\alpha\delta}\delta_{\gamma\beta}}{4} \right). \quad (104)$$

This result is not symmetric (it is reminded by the tilde above the  $\sigma$  symbol). Symmetrizing it according to the rule (95) we get

$$\underbrace{\sigma_{\alpha\beta\gamma\delta}^{(3)}(\omega_1, \omega_2, \omega_3)}_{(1/2)} \approx \sigma_0^{(3)} \frac{i}{6} \frac{\delta_{\alpha\beta}\delta_{\gamma\delta} + \delta_{\alpha\gamma}\delta_{\beta\delta} + \delta_{\alpha\delta}\delta_{\gamma\beta}}{(\Omega_1 + i\Gamma)(\Omega_2 + i\Gamma)(\Omega_3 + i\Gamma)}. \quad (105)$$

The correction to (105) is again of order  $O(1/\Omega^5)$ . Now consider the last, (0/3) contribution. The function  $\mathcal{K}(z)$  at large  $|z| = |\Omega + i\Gamma|$  has the asymptote

$$\mathcal{K}(z) \approx \frac{1}{z} - \frac{i\pi}{z^2} + O\left(\frac{1}{z^3}\right). \quad (106)$$

Substituting (106) into Eq. (94) we see that, apart from the  $O(1/\Omega^3)$  contribution, the term (0/3) has the correction of order  $O(1/\Omega^4)$ . Calculating, first, only the  $\Omega^{-3}$  contribution we get

$$\underbrace{\sigma_{\alpha\beta\gamma\delta}^{(3)}(\omega_1, \omega_2, \omega_3)}_{(0/3)} \approx \sigma_0^{(3)} \frac{i}{6} \frac{\delta_{\alpha\beta}\delta_{\gamma\delta} + \delta_{\alpha\gamma}\delta_{\beta\delta} + \delta_{\alpha\delta}\delta_{\beta\gamma}}{(\Omega_1 + i\Gamma)(\Omega_2 + i\Gamma)(\Omega_3 + i\Gamma)} + \dots, \quad (107)$$

where the omitted term is of order  $O(1/\Omega^4)$ . Collecting now all the  $\Omega^{-3}$  contributions (91), (103), (105) and (107), we see that they cancel out. The main contribution to the third-order conductivity at large frequencies is thus of order  $O(1/\Omega^4)$  and comes from the *purely inter-band* contribution (0/3) (all other corrections are of order  $O(1/\Omega^5)$ ). In the non-symmetrized form it reads

$$\begin{aligned} \tilde{\sigma}_{\alpha\beta\gamma\delta}^{(3)}(\omega_1, \omega_2, \omega_3) &\approx i\sigma_0^{(3)} \left( \delta_{\alpha\beta}\delta_{\gamma\delta} + \delta_{\alpha\gamma}\delta_{\beta\delta} + \delta_{\alpha\delta}\delta_{\beta\gamma} \right) \\ &\times (-i\pi) \frac{(\Omega_1 + \Omega_2 + \Omega_3 + i3\Gamma) \frac{1}{(\Omega_1 + i\Gamma)^2} - (\Omega_1 + i\Gamma) \frac{1}{(\Omega_1 + \Omega_2 + \Omega_3 + i3\Gamma)^2}}{(\Omega_1 + \Omega_2 + i2\Gamma)(2\Omega_1 + \Omega_2 + \Omega_3 + i4\Gamma)(\Omega_2 + \Omega_3 + i2\Gamma)}, \end{aligned} \quad (108)$$

If  $\Gamma \rightarrow 0$  this contribution is purely real and results from the imaginary parts of the logarithmic functions in (94) which physically corresponds to the single-photon ( $\hbar\omega_j \simeq 2E_F$ ) and three-photon [ $\hbar(\omega_1 + \omega_2 + \omega_3) \simeq 2E_F$ ] absorption at the inter-band absorption edge. Symmetrizing Eq. (108) we finally get the following expression for the third-order conductivity at large frequencies  $|\Omega_j + i\Gamma|/2 \gg 1$ :

$$\begin{aligned} \sigma_{\alpha\beta\gamma\delta}^{(3)}(\omega_1, \omega_2, \omega_3) &\approx \sigma_0^{(3)} \frac{\delta_{\alpha\beta}\delta_{\gamma\delta} + \delta_{\alpha\gamma}\delta_{\beta\delta} + \delta_{\alpha\delta}\delta_{\beta\gamma}}{6} \\ &\times \left\{ \frac{1}{(\Omega_1 + \Omega_2 + \Omega_3 + i3\Gamma)} \left( \frac{1}{(\Omega_1 + i\Gamma)(\Omega_1 + \Omega_2 + i2\Gamma)(\Omega_1 + \Omega_3 + i2\Gamma)} \right. \right. \end{aligned}$$

$$\begin{aligned}
& + \frac{1}{(\Omega_2 + i\Gamma)(\Omega_1 + \Omega_2 + i2\Gamma)(\Omega_2 + \Omega_3 + i2\Gamma)} + \frac{1}{(\Omega_3 + i\Gamma)(\Omega_3 + \Omega_1 + i2\Gamma)(\Omega_3 + \Omega_2 + i2\Gamma)} \Big) \\
& + \left( \frac{1}{(\Omega_1 + i\Gamma)^2(\Omega_1 + \Omega_2 + i2\Gamma)(\Omega_1 + \Omega_3 + i2\Gamma)} + \frac{1}{(\Omega_2 + i\Gamma)^2(\Omega_1 + \Omega_2 + i2\Gamma)(\Omega_2 + \Omega_3 + i2\Gamma)} \right. \\
& \quad \left. + \frac{1}{(\Omega_3 + i\Gamma)^2(\Omega_3 + \Omega_1 + i2\Gamma)(\Omega_3 + \Omega_2 + i2\Gamma)} \right) \\
& + \frac{2}{(\Omega_1 + \Omega_2 + i2\Gamma)(\Omega_1 + \Omega_3 + i2\Gamma)(\Omega_2 + \Omega_3 + i2\Gamma)(\Omega_1 + \Omega_2 + \Omega_3 + i3\Gamma)} \Big\}, \quad |\Omega_j + i\Gamma|/2 \gg 1; \\
\end{aligned} \tag{109}$$

corrections to (109) are of order  $1/\Omega^5$ . Thus, while at low frequencies  $\Omega \ll 2$  the third conductivity drops as  $1/\Omega^3$ , at high frequencies  $\Omega \gg 2$  it goes down even faster, as  $1/\Omega^4$ . Notice that, since  $\sigma_0^{(3)} \propto 1/E_F^4$  and  $(\Omega_j + i\Gamma) = \hbar(\omega_j + i\gamma)/E_F$ , the asymptote (109) does not depend on the Fermi energy as it should be. The formula (109) can be used for analyzing experimental results on the nonlinear *optical* response of a single graphene layer if all involved frequencies exceed  $2E_F/\hbar$ .

Let us estimate the absolute values of  $\sigma^{(3)}$  and  $\chi^{(3)}$  of graphene at optical frequencies. Assuming that all frequencies are the same and the  $\Gamma$  parameter is small,  $\Omega_j \approx \Omega \gg \Gamma$  we get for  $\sigma_{xxxx}^{(3)}(\omega, \omega, \omega)$ :

$$\sigma_{xxxx}^{(3)}(\omega, \omega, \omega) \simeq \frac{e^4 \hbar v_F^2}{8E_F^4} \frac{1}{\Omega^4} \left( \frac{1}{4} + \frac{3}{4} + \frac{1}{12} \right) = \frac{e^4 v_F^2}{8\hbar^3 \omega^4} \frac{13}{12}. \tag{110}$$

The factors  $1/4$ ,  $3/4$  and  $1/12$  come from the first and second, third and forth, and the fifth lines in (109), respectively. Substituting  $v_F = 10^8$  cm/s we get at the wavelength  $\lambda = 2\pi c/\omega = 1 \mu\text{m}$

$$\sigma_{xxxx}^{(3)}(\omega, \omega, \omega) \simeq 4.9 \times 10^{-3} \text{ esu} \text{ and } \chi_{xxxx}^{(3)}(\omega, \omega, \omega) \simeq 7.9 \times 10^{-11} \text{ esu}, \tag{111}$$

where we have used electrostatic units. It should be emphasized that the numbers (102), (111) are obtained for an isolated graphene layer; in a real experimental situation, when the graphene layer lies on a dielectric (or other) substrate, the corresponding numbers can be substantially different.

The optical-frequencies result (109) can be directly compared with the one given by Cheng et al. in Ref.<sup>32</sup> (see Eq. (2) there). The result found in Ref.<sup>32</sup> coincides with the very last (fifth) line in (109). The contributions presented by the first four lines in the brackets in (109) are absent in Ref.<sup>32</sup>. Notice that numerically the fifth-line contribution is less than 10% of the whole value of  $\sigma^{(3)}$ , see the corresponding contributions in Eq. (110).

### C. Resonances at $\hbar\omega \simeq 2E_F$

A very important result of this work (as well as of Ref.<sup>28</sup>) is that the third-order response of graphene demonstrates a strong resonance at the frequencies  $\hbar\omega_j \simeq 2E_F$  which in the linear-response regime corresponds to the inter-band absorption edge. The linear response conductivity shows only a step-like feature in the real part of  $\sigma^{(1)}$  and a relatively weak (logarithmic) ‘‘divergence’’ (hidden by the finite scattering rate  $\gamma$ ) in the imaginary part of  $\sigma^{(1)}$ , see Figures 2(b),(c). In contrast, in the third-order conductivity we have the second-order pole at  $\hbar\omega \simeq 2E_F$  which allows one to get a strong, resonant enhancement of the third-order effects at the frequencies corresponding to the condition  $\omega \simeq 2E_F/\hbar$ . This resonance is electrically tunable in the range from about 10 to 300 THz (the wavelength from 1 to 30  $\mu\text{m}$ ), see Figure 3, at the electron densities varying from  $\simeq 0.3 \times 10^{11}$  to  $\simeq 3 \times 10^{13} \text{ cm}^{-2}$ . This resonantly increases the efficiency of the third-order effects and makes graphene especially attractive for the creation of electrically controlled nonlinear electronic and optoelectronic devices operating in the broad near-infrared – far-infrared frequency range.

Consider the vicinity of the  $2E_F$  resonances more closely. As seen from the summary of results (91) – (94), the quasi-classical (3/0) contribution does not have any resonant feature at  $\Omega_j \simeq 2$ , the (2/1) and (1/2) contributions have the poles of the second and first orders respectively, and the purely quantum inter-band term (3/0) has the logarithmic feature around  $\Omega_j \simeq 2$ . The strength of the resonance falls down from (2/1) to (3/0) terms, so that the largest contribution at  $\Omega_j \simeq 2$  is given by the term (2/1), resulting from the summands with two intra-band and one

inter-band matrix elements. Near the points  $\Omega_j \simeq 2$  we get from Eq. (92) the non-symmetrized form of the third conductivity:

$$\tilde{\sigma}_{\alpha\beta\gamma\delta}^{(3)}(\omega_1, \omega_2, \omega_3) \approx i\sigma_0^{(3)} \frac{4\delta_{\alpha\delta}\delta_{\beta\gamma} - [\delta_{\alpha\beta}\delta_{\gamma\delta} + \delta_{\alpha\gamma}\delta_{\beta\delta} + \delta_{\alpha\delta}\delta_{\beta\gamma}]}{8(\Omega_1 + i\Gamma)(\Omega_2 + i\Gamma)[1 - (\Omega_3 + i\Gamma)/2]^2}. \quad (112)$$

After the symmetrization according to (95) we get near the  $2E_F$  resonance:

$$\begin{aligned} \sigma_{\alpha\beta\gamma\delta}^{(3)}(\omega_1, \omega_2, \omega_3) \approx \sigma_0^{(3)} \frac{i}{24} \left\{ \frac{4\delta_{\alpha\delta}\delta_{\beta\gamma} - [\delta_{\alpha\beta}\delta_{\gamma\delta} + \delta_{\alpha\gamma}\delta_{\beta\delta} + \delta_{\alpha\delta}\delta_{\beta\gamma}]}{(\Omega_1 + i\Gamma)(\Omega_2 + i\Gamma)[1 - (\Omega_3 + i\Gamma)/2]^2} \right. \right. \\ \left. \left. + \frac{4\delta_{\alpha\gamma}\delta_{\beta\delta} - [\delta_{\alpha\beta}\delta_{\gamma\delta} + \delta_{\alpha\gamma}\delta_{\beta\delta} + \delta_{\alpha\delta}\delta_{\beta\gamma}]}{(\Omega_1 + i\Gamma)(\Omega_3 + i\Gamma)[1 - (\Omega_2 + i\Gamma)/2]^2} + \frac{4\delta_{\alpha\beta}\delta_{\gamma\delta} - [\delta_{\alpha\beta}\delta_{\gamma\delta} + \delta_{\alpha\gamma}\delta_{\beta\delta} + \delta_{\alpha\delta}\delta_{\beta\gamma}]}{(\Omega_2 + i\Gamma)(\Omega_3 + i\Gamma)[1 - (\Omega_1 + i\Gamma)/2]^2} \right\}. \quad (113) \right. \end{aligned}$$

Let us estimate now the absolute value of  $\sigma^{(3)}$  near the  $2E_F$  resonance. Assume that all frequencies are the same,  $\Omega_1 = \Omega_2 = \Omega_3 = \Omega \approx 2$  and  $\Gamma \ll 1$ . Then we have from (113) for  $\sigma_{xxxx}^{(3)}(\omega, \omega, \omega)$ :

$$\sigma_{xxxx}^{(3)}(\omega, \omega, \omega) \approx \sigma_0^{(3)} \frac{i}{8} \frac{1}{\Omega^2[1 - (\Omega + i\Gamma)/2]^2} \approx -\frac{ie^4 \hbar v_F^2}{8\pi E_F^4} \frac{1}{4\Gamma^2}. \quad (114)$$

Comparing the result (114) at the vicinity of the resonance  $\hbar\omega \simeq 2E_F$  with the non-resonant value of  $\sigma^{(3)}$  in Eq. (110) we see that the third-order conductivity at the resonance increases by a factor

$$\frac{\sigma_{\text{res}}^{(3)}}{\sigma_{\text{non-res}}^{(3)}} \simeq \frac{48}{13\pi\Gamma^2} \simeq \frac{1.175}{\Gamma^2}. \quad (115)$$

If the density of electrons is  $n_s \simeq 2.8 \times 10^{13} \text{ cm}^{-2}$  which corresponds to the resonance at  $\lambda = 1 \mu\text{m}$ , and the scattering parameter  $\gamma \simeq 10^{12} \text{ s}^{-1}$ , the factor  $\Gamma = \hbar\gamma/E_F$  is about  $10^{-3}$ , so that the right-hand side of Eq. (115) is about  $10^6$ . The effective  $\chi^{(3)}$ , see Eq. (111), would then be about  $8 \times 10^{-5} \text{ esu}$  at  $\lambda \simeq 1 \mu\text{m}$ , which is enormously high value for nonlinear materials.

#### D. Logarithmic feature at $\hbar\omega \simeq 2E_F/3$

As seen from the general results (91) – (94), apart from the resonance at  $\hbar\omega \simeq 2E_F$  the third-order frequency response also contains a logarithmic feature at  $\hbar(\omega_1 + \omega_2 + \omega_3) \simeq 2E_F$ . This purely quantum feature, which physically corresponds to a three-photon absorption and comes from the (0/3) contribution (94), is much weaker than the strong (partly classical) resonance at  $\hbar\omega \simeq 2E_F$ .

The behavior of the third-order conductivity near the points  $\hbar(\omega_1 + \omega_2 + \omega_3) \simeq 2E_F$  can be obtained from Eq. (94) since only the (0/3) term contains the logarithmic feature near this point. Assuming for simplicity that  $\Omega_1 = \Omega_2 = \Omega_3 = \Omega \approx 2/3$  and  $\Gamma \ll 1$  we get:

$$\begin{aligned} \sigma_{\alpha\beta\gamma\delta}^{(3)}(\omega, \omega, \omega) \approx i\sigma_0^{(3)} \left( \delta_{\alpha\beta}\delta_{\gamma\delta} + \delta_{\alpha\gamma}\delta_{\beta\delta} + \delta_{\alpha\delta}\delta_{\beta\gamma} \right) \frac{3\mathcal{K}(\Omega + i\Gamma) - \mathcal{K}(3(\Omega + i\Gamma))}{16(\Omega + i\Gamma)^2} \\ \approx i\sigma_0^{(3)} \left( \delta_{\alpha\beta}\delta_{\gamma\delta} + \delta_{\alpha\gamma}\delta_{\beta\delta} + \delta_{\alpha\delta}\delta_{\beta\gamma} \right) \frac{9}{256} \left( 16 - 25 \ln 2 - \ln[2 - 3(\Omega + i\Gamma)] \right); \quad (116) \end{aligned}$$

(in all places except in the logarithm we have substituted  $\Omega = 2/3$ ). Exactly at the point  $\Omega = 2/3$  we have

$$\sigma_{\alpha\beta\gamma\delta}^{(3)}(\omega, \omega, \omega) \approx i\sigma_0^{(3)} \left( \delta_{\alpha\beta}\delta_{\gamma\delta} + \delta_{\alpha\gamma}\delta_{\beta\delta} + \delta_{\alpha\delta}\delta_{\beta\gamma} \right) \mathcal{N} \quad (117)$$

with  $\mathcal{N}$  being a numerical factor which is very small even at  $\Gamma \simeq 10^{-3}$ :

$$\mathcal{N} = \frac{9}{256} \left( 16 - 25 \ln 2 - \ln(-i3\Gamma) \right) \approx 0.1575 + 0.0552i \text{ at } \Gamma = 10^{-3}. \quad (118)$$

In most experimentally relevant situations the logarithmic feature at  $\hbar\omega = 2E_F/3$  is thus of no (or little) importance.

It should be noticed, again, that the results of Cheng et al., Refs.<sup>32–34</sup>, strongly disagree with ours. For example, Figure 1(b) in Ref.<sup>32</sup> shows a strong resonance of  $\sigma_{xxxy}^{(3)}(\omega, \omega, \omega)$  at  $\hbar\omega \simeq 2E_F/3$ , a slightly weaker one at  $\hbar\omega \simeq E_F$  and no resonance at all at  $\hbar\omega \simeq 2E_F$ . In our theory the second-order-pole single-photon feature at  $\hbar\omega = 2E_F$  is much stronger than the logarithmic three-photon feature at  $\hbar\omega = 2E_F/3$ , and there is no resonance at the two-photon absorption  $\hbar\omega \simeq E_F$  (this is seen already in formulas (53) – (56)).

## VI. THIRD-ORDER RESPONSE TO A MONOCHROMATIC EXCITATION

Now we consider the third-order response of a graphene monolayer to an external monochromatic radiation with the frequency  $\omega$ . The results for the third-harmonic generation at the linear polarization of the incident electromagnetic wave have been briefly presented in Ref.<sup>28</sup>. Here we discuss the generation of the  $3\omega$ -harmonic in some more detail, including the case of the elliptic polarization, and study the optical Kerr effect, i.e. the current response at the same frequency  $\omega$ . The latter effect leads, for example, to the absorption of saturation which is especially pronounced when the incident wave frequency is close to the absorption edge  $\hbar\omega = 2E_F$ .

### A. Third harmonic generation, linear polarization

#### 1. Third-order conductivity

Let the external electromagnetic radiation be linearly polarized in the  $x$ -direction and have only one frequency harmonic,

$$E_\alpha(t) = E_0 \delta_{x\alpha} \cos \omega t. \quad (119)$$

Then the Fourier component of the field is

$$E_{\omega_1}^\beta = \frac{1}{2} E_0 \delta_{x\beta} \left( \delta(\omega_1 - \omega) + \delta(\omega_1 + \omega) \right) \quad (120)$$

and the current (60) assumes the form

$$j_\alpha^{(3)}(t) = \frac{1}{8} E_0^3 \left( \sigma_{\alpha x x x}^{(3)}(\omega, \omega, \omega) e^{-i3\omega t} + \left( \sigma_{\alpha x x x}^{(3)}(\omega, \omega, -\omega) + \sigma_{\alpha x x x}^{(3)}(\omega, -\omega, \omega) + \sigma_{\alpha x x x}^{(3)}(-\omega, \omega, \omega) \right) e^{-i\omega t} + \text{c.c.} \right), \quad (121)$$

where c.c. means the complex conjugate. Since  $\sigma_{y x x x}^{(3)}$  equals zero, the current is polarized in the same ( $x$ -) direction and its absolute value at the frequency  $3\omega$  is determined by the third-order conductivity  $\sigma_{x x x x}^{(3)}(\omega, \omega, \omega)$ . Using the general results (89) – (95) we get

$$\sigma_{\alpha\beta\gamma\delta}^{(3)}(\omega, \omega, \omega) = \sigma_0^{(3)} \left( \mathcal{S}_{\alpha\beta\gamma\delta}^{(3/0)}(\Omega, \Omega, \Omega) + \tilde{\mathcal{S}}_{\alpha\beta\gamma\delta}^{(2/1)}(\Omega, \Omega, \Omega) + \tilde{\mathcal{S}}_{\alpha\beta\gamma\delta}^{(1/2)}(\Omega, \Omega, \Omega) + \tilde{\mathcal{S}}_{\alpha\beta\gamma\delta}^{(0/3)}(\Omega, \Omega, \Omega) \right), \quad (122)$$

where

$$\mathcal{S}_{\alpha\beta\gamma\delta}^{(3/0)}(\Omega, \Omega, \Omega) = i \frac{\delta_{\alpha\beta}\delta_{\gamma\delta} + \delta_{\alpha\gamma}\delta_{\beta\delta} + \delta_{\alpha\delta}\delta_{\beta\gamma}}{6(\Omega + i\Gamma)^3}, \quad (123)$$

$$\begin{aligned} \tilde{\mathcal{S}}_{\alpha\beta\gamma\delta}^{(2/1)}(\Omega, \Omega, \Omega) &= \frac{i}{2(\Omega + i\Gamma)^2} \left\{ \delta_{\alpha\delta}\delta_{\beta\gamma} \left( \frac{1}{[1 - (\Omega + i\Gamma)/2]^2} - \frac{1}{[1 + (\Omega + i\Gamma)/2]^2} \right) \right. \\ &\quad \left. - \frac{\delta_{\alpha\beta}\delta_{\gamma\delta} + \delta_{\alpha\gamma}\delta_{\beta\delta} + \delta_{\alpha\delta}\delta_{\beta\gamma}}{4} \left( \frac{(\Omega + i\Gamma)/2}{[1 + (\Omega + i\Gamma)/2]^2} + \frac{(\Omega + i\Gamma)/2}{[1 - (\Omega + i\Gamma)/2]^2} \right) \right\}, \end{aligned} \quad (124)$$

$$\tilde{\mathcal{S}}_{\alpha\beta\gamma\delta}^{(1/2)}(\Omega, \Omega, \Omega) = \frac{i}{2(\Omega + i\Gamma)^2} \left( \frac{1}{1 + (\Omega + i\Gamma)/2} - \frac{1}{1 - (\Omega + i\Gamma)/2} \right) \left( \delta_{\alpha\beta}\delta_{\gamma\delta} - \frac{\delta_{\alpha\beta}\delta_{\gamma\delta} + \delta_{\alpha\gamma}\delta_{\beta\delta} + \delta_{\alpha\delta}\delta_{\beta\gamma}}{4} \right), \quad (125)$$

and

$$\begin{aligned} \tilde{\mathcal{S}}_{\alpha\beta\gamma\delta}^{(0/3)}(\Omega, \Omega, \Omega) &= i \left( \delta_{\alpha\beta}\delta_{\gamma\delta} + \delta_{\alpha\gamma}\delta_{\beta\delta} + \delta_{\alpha\delta}\delta_{\beta\gamma} \right) \frac{3\mathcal{K}(\Omega + i\Gamma) - \mathcal{K}(3(\Omega + i\Gamma))}{16(\Omega + i\Gamma)^2} \\ &= i \frac{\delta_{\alpha\beta}\delta_{\gamma\delta} + \delta_{\alpha\gamma}\delta_{\beta\delta} + \delta_{\alpha\delta}\delta_{\beta\gamma}}{6(\Omega + i\Gamma)^3} \left[ 1 + \frac{9}{8(\Omega + i\Gamma)} \left( \ln \frac{2 - (\Omega + i\Gamma)}{2 + (\Omega + i\Gamma)} - \frac{1}{3^3} \ln \frac{2 - 3(\Omega + i\Gamma)}{2 + 3(\Omega + i\Gamma)} \right) \right]. \end{aligned} \quad (126)$$

If  $\alpha\beta\gamma\delta \neq xxxx$ , the formulas (124) and (125) should be symmetrized according to the rule (95).

Figure 4 shows the contributions (123) – (126), at  $\alpha\beta\gamma\delta = xxxx$ , as a function of frequency  $\Omega$ . The following features are seen:

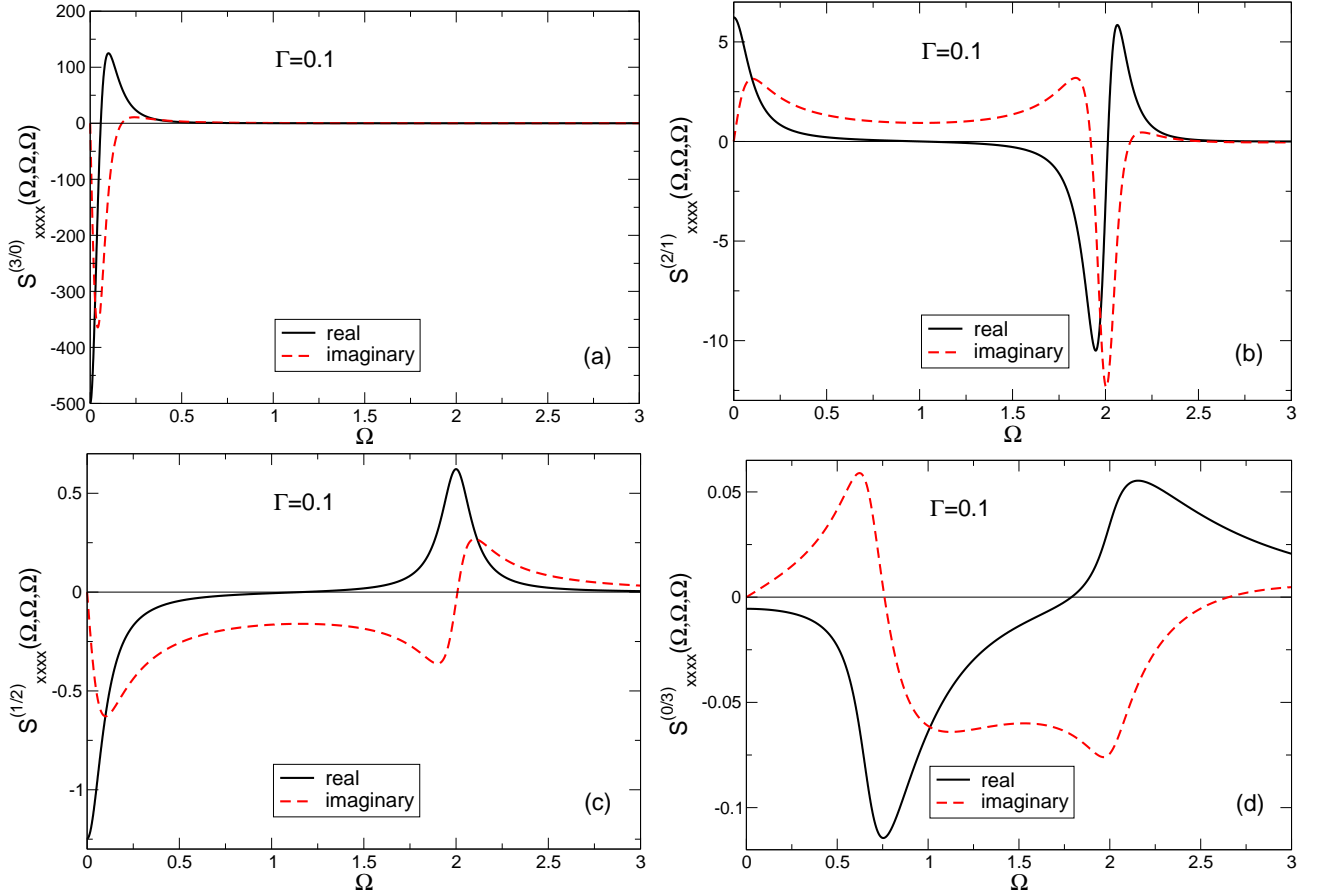


FIG. 4: Four contributions to the third order conductivity  $\sigma_{xxxx}^{(3)}(\omega, \omega, \omega)/\sigma_0^{(3)}$ , where  $\sigma_0^{(3)}$  is defined in (68): (a) (3/0) contribution, (b) (2/1) contribution, (c) (1/2) contribution, (d) (0/3) contribution. The effective scattering parameter is  $\Gamma = 0.1$ .

1. The classical (3/0) contribution has a large resonance at low frequencies  $\Omega \lesssim \Gamma$ . The contributions (2/1) and (1/2), determined by both the classical (intra-band) and quantum (inter-band) matrix elements, have resonances both at low ( $\Omega \lesssim \Gamma$ ) and at high frequency ( $\Omega \simeq 2$ ) corresponding to the single-photon absorption edge due to the quantum inter-band transition. The purely quantum contribution (0/3) has no resonance at low frequencies but has logarithmic features at the frequencies of the single-photon ( $\Omega \simeq 2$ ) and triple-photon ( $\Omega \simeq 2/3$ ) inter-band transitions.
2. The absolute values of the different contributions to the third-order conductivity gradually decrease from the purely classical (3/0) to the purely quantum (0/3) contributions: at  $\Gamma = 0.1$  the scale of the (3/0) term is about 500, of the (2/1) term – about 10, of the (1/2) term about 1 and of the (0/3) contribution – about 0.1. The largest contribution at low (microwave, terahertz) frequencies is thus expected from the classical term (3/0), while the largest contribution at high (infrared/optical) frequencies is expected at the resonance  $\Omega = 2$  ( $\hbar\omega = 2E_F$ ) from the (2/1) contribution. This fact has been already discussed in Section V.

Figure 5 shows the total third-order conductivity at  $\Gamma = 0.01$  in different frequency ranges. The logarithmic feature at  $\Omega = 2/3$  is very weak and almost invisible, while the resonances at  $\Omega \lesssim \Gamma$  and  $\Omega \simeq 2$  are very strong. They can be used for creation of different voltage tunable devices at terahertz and infrared/optical frequencies.

## 2. *Emitted power density at the third harmonic*

Let us consider an isolated (hanging) graphene layer in free space irradiated by an incident electromagnetic wave with the frequency  $\omega$  and the intensity  $I_\omega$ . Let the field of the incident wave is described by Eq. (119) so that the

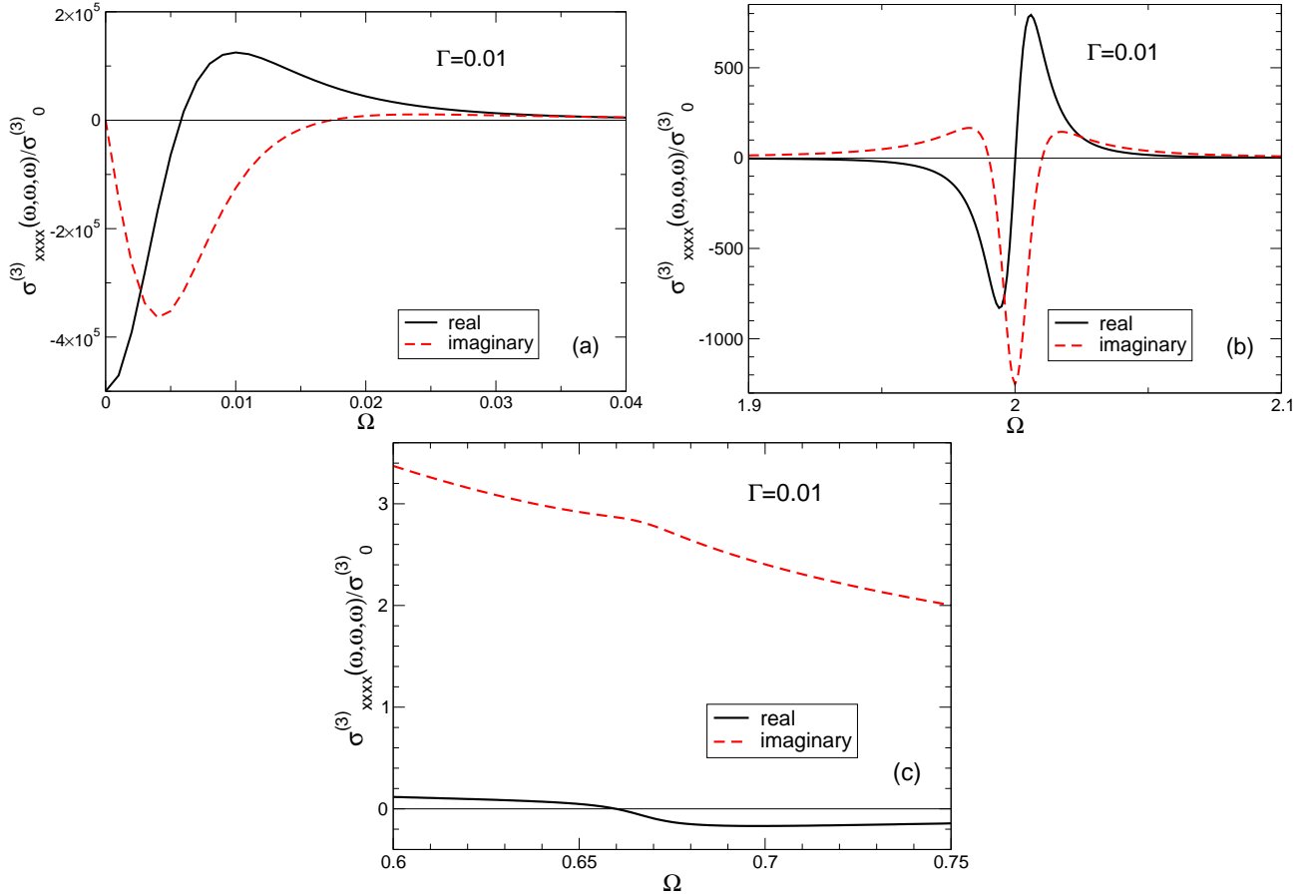


FIG. 5: The total third order conductivity  $\sigma_{xxx}^{(3)}(\omega, \omega, \omega)/\sigma_0^{(3)}$  (a) at low-frequencies  $\Omega \lesssim \Gamma$ , (b) near the high-frequency resonance at  $\Omega \simeq 2$ , and (c) near the logarithmic feature at  $\Omega \simeq 2/3$ . The effective scattering parameter is  $\Gamma = 0.01$ .

Fourier component is  $E_\omega = E_0/2$ . Ignoring for simplicity the self-consistent screening effect we have

$$I_\omega = \frac{c}{2\pi} |E_\omega|^2 = \frac{c}{8\pi} E_0^2. \quad (127)$$

The Fourier component of the induced third-harmonic current is, according to (121),

$$j_{3\omega}^{(3)} = \sigma_{xxx}^{(3)}(\omega, \omega, \omega) E_\omega^3 = \sigma_{xxx}^{(3)}(\omega, \omega, \omega) \left( \frac{E_0}{2} \right)^3. \quad (128)$$

The Fourier amplitudes of the third-harmonic electric and magnetic fields are then

$$E_{3\omega} = H_{3\omega} = \frac{2\pi}{c} j_{3\omega}^{(3)} = \frac{2\pi}{c} \sigma_{xxx}^{(3)}(\omega, \omega, \omega) E_\omega^3, \quad (129)$$

and the intensity of the emitted third-harmonic radiation is

$$I_{3\omega} = \frac{c}{2\pi} |E_{3\omega}|^2 = \left( \frac{2\pi}{c} \right)^4 \left| \sigma_{xxx}^{(3)}(\omega, \omega, \omega) \right|^2 I_\omega^3. \quad (130)$$

This can be written as

$$\frac{I_{3\omega}}{I_\omega} = \left( \frac{e^4}{\hbar^2 c^2} \frac{I_\omega}{\pi n_s^2 \hbar v_F^2} \right)^2 \left| \mathcal{S}_{xxx}^{(3/0)}(\Omega, \Omega, \Omega) + \mathcal{S}_{xxx}^{(2/1)}(\Omega, \Omega, \Omega) + \mathcal{S}_{xxx}^{(1/2)}(\Omega, \Omega, \Omega) + \mathcal{S}_{xxx}^{(0/3)}(\Omega, \Omega, \Omega) \right|^2. \quad (131)$$

Figure 6 shows the ratio (131) as a function of the electron density at a few values of the input-wave wavelengths for a single graphene layer hanging in vacuum. The input power density is assumed to be  $I_\omega = 1 \text{ MW/cm}^2$  and

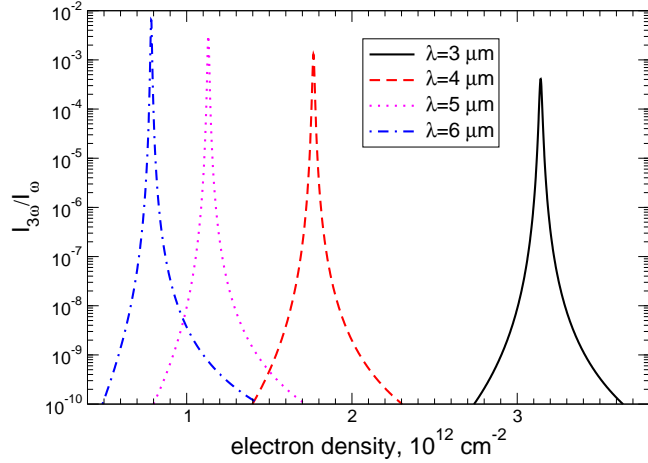


FIG. 6: The up-conversion efficiency  $I_{3\omega}/I_\omega$ , Eq. (131) at the incident wave power density  $I_\omega = 1 \text{ MW/cm}^2$  and the effective scattering time  $\tau = 1 \text{ ps}$  for an isolated graphene layer in vacuum.  $\lambda$  is the wavelength of the *incident* wave; the corresponding output (third-harmonic)  $\lambda$ 's are 1, 1.33, 1.67, and 2  $\mu\text{m}$  respectively.

the effective scattering time  $\tau = 1/\gamma = 1 \text{ ps}$ . One sees that at the input radiation wavelength of  $\lambda_\omega = 6 \mu\text{m}$  the up-conversion efficiency can be as large as  $\sim 1\%$  under these conditions which corresponds to the output power density of about  $10 \text{ kW/cm}^2$  at the wavelength  $\lambda_{3\omega} = \lambda_\omega/3 = 2 \mu\text{m}$ . At the shorter wavelengths the up-conversion efficiency decreases but it can be made bigger at the larger incident wave intensity  $I_\omega$ . Notice also that the resonances at  $\hbar\omega = 2E_F$  are very sharp which can be used for a fine electrical tuning of the graphene based frequency multipliers.

### B. Third harmonic generation, elliptic polarization

Consider the case of an elliptic polarization of the external field,

$$E_\alpha(t) = \delta_{\alpha x} E_a \cos \omega t + \delta_{\alpha y} E_b \sin \omega t. \quad (132)$$

Substituting the Fourier components of the field

$$E_{\omega_1}^\alpha = \delta_{\alpha x} \frac{E_a}{2} \left( \delta(\omega_1 - \omega) + \delta(\omega_1 + \omega) \right) + \delta_{\alpha y} \frac{E_b}{2i} \left( \delta(\omega_1 - \omega) - \delta(\omega_1 + \omega) \right) \quad (133)$$

in the third-order current (60) we get at the frequency  $3\omega$ :

$$j_{\alpha,3\omega}^{(3)}(t) = \frac{1}{8} \sigma_{xxxx}^{(3)}(\omega, \omega, \omega) \left( E_a^2 - E_b^2 \right) \left( \delta_{\alpha x} E_a - i \delta_{\alpha y} E_b \right) e^{-i3\omega t} + \text{c.c.}; \quad (134)$$

deriving this equation we have used the relations (97) – (98). At the elliptic polarization of the incident wave the frequency dependence of the third-order current is thus determined by the same function  $\sigma_{xxxx}^{(3)}(\omega, \omega, \omega)$ , Figures 4 – 5, but the amplitude of the current is smaller. In particular, at the circular polarization,  $E_a = E_b$ , the current  $j_{\alpha,3\omega}^{(3)}(t)$  vanishes.

### C. Third-order response at the incident-wave frequency: the absorption saturation

Now consider the third-order response of graphene to the linearly polarized external electromagnetic radiation at the frequency of the incident wave  $\omega$ . The corresponding current contribution is polarized in the  $x$ -direction and is given by the term proportional to  $e^{-i\omega t}$  in Eq. (121). Using the symmetry of  $\sigma_{xxxx}^{(3)}$  we get

$$j_{x,\omega}^{(3)}(t) = \frac{3}{8} E_0^3 \sigma_{xxxx}^{(3)}(\omega, \omega, -\omega) e^{-i\omega t} + \text{c.c..} \quad (135)$$

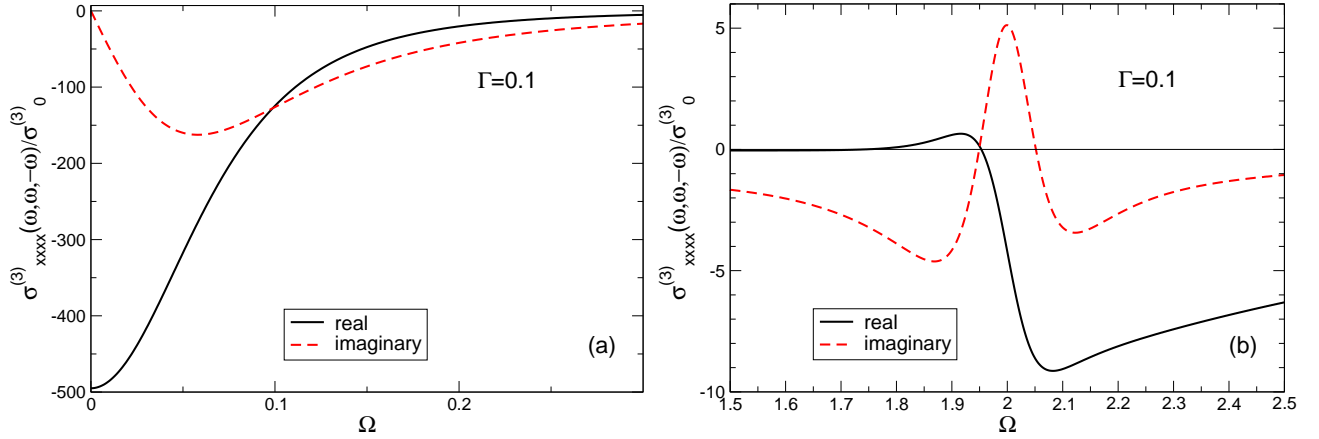


FIG. 7: The third-order conductivity  $\sigma_{xxxx}^{(3)}(\omega, \omega, -\omega)/\sigma_0^{(3)}$  as a function of frequency  $\Omega$  at  $\Gamma = 0.1$  in the regime of (a) low ( $\Omega \ll 1$ ) and (b) high ( $\Omega \simeq 2$ ) frequencies.

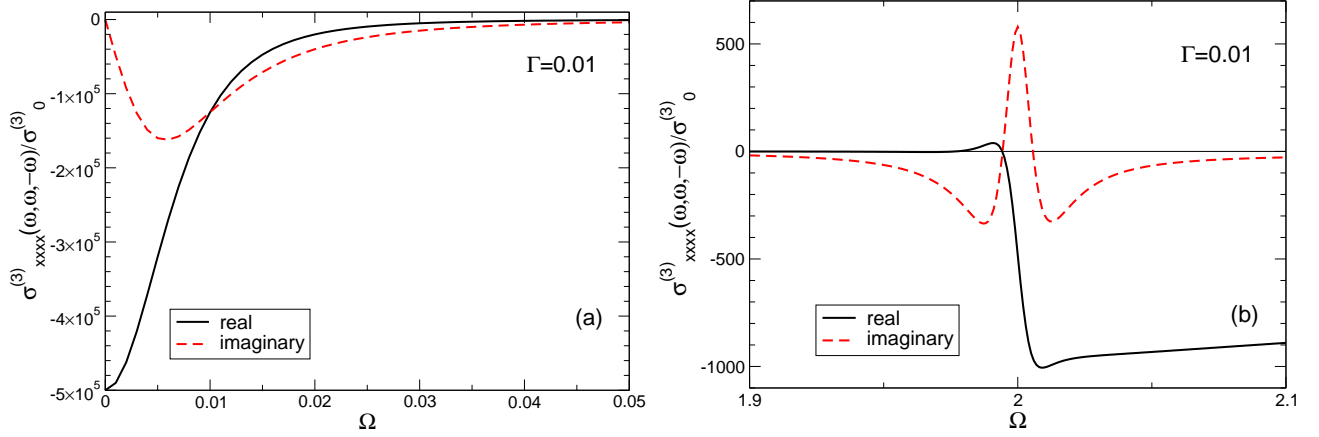


FIG. 8: The same as in Figure 7 but at  $\Gamma = 0.01$ .

Figures 7 and 8 show the third-order conductivity  $\sigma_{xxxx}^{(3)}(\omega, \omega, -\omega)/\sigma_0^{(3)}$  as a function of frequency in the low- (microwave/terahertz) and high- (infrared/visible) frequency range. Again, one sees a strong resonance at low frequencies and a weaker but sharp resonance at  $\Omega \simeq 2$ .

The third-order current contribution (135) can be added to the linear-response current, Eq. (43), to get the electric-field dependent response of graphene at the frequency  $\omega$ . In up to the third order in the electric field we have

$$j_{x,\omega}(t) \approx \frac{1}{2} E_0 \left[ \sigma_{xx}^{(1)}(\omega) + \frac{3}{4} E_0^2 \sigma_{xxxx}^{(3)}(\omega, \omega, -\omega) \right] e^{-i\omega t} + \text{c.c.} \equiv \frac{1}{2} \sigma_{xx}(\omega, E_0) E_0 e^{-i\omega t} + \text{c.c.} \quad (136)$$

The corresponding field-dependent dynamic conductivity is then

$$\begin{aligned} \sigma_{xx}(\omega, E_0) &= \sigma_{xx}^{(1)}(\omega) + \frac{3}{4} E_0^2 \sigma_{xxxx}^{(3)}(\omega, \omega, -\omega) \\ &= \sigma_0^{(1)} \left[ \mathcal{S}_{xx}^{(1)}(\Omega) + \frac{3}{4\pi} \left( \frac{eE_0}{E_F k_F} \right)^2 \mathcal{S}_{xxxx}^{(3)}(\Omega, \Omega, -\Omega) \right] \end{aligned} \quad (137)$$

where the functions  $\mathcal{S}_{\alpha\beta}^{(1)}(\Omega)$  and  $\mathcal{S}_{\alpha\beta\gamma\delta}^{(3)}(\Omega_1, \Omega_2, \Omega_3)$  are defined in (45) – (47) and (90) – (94), respectively. The dimensionless field parameter  $eE_0/E_F k_F$  in (137) is the work of the field, performed on 2D electrons at the length  $\sim k_F^{-1}$ , divided by their average (Fermi) energy. Figure 9 shows the absorption coefficient of an isolated graphene layer with the field-dependent conductivity (137) at low ( $\Omega \ll 1$ ) and high ( $\Omega \simeq 2$ ) frequencies. The absorption is seen to be substantially suppressed at the external electric field parameter exceeding a certain value which depends

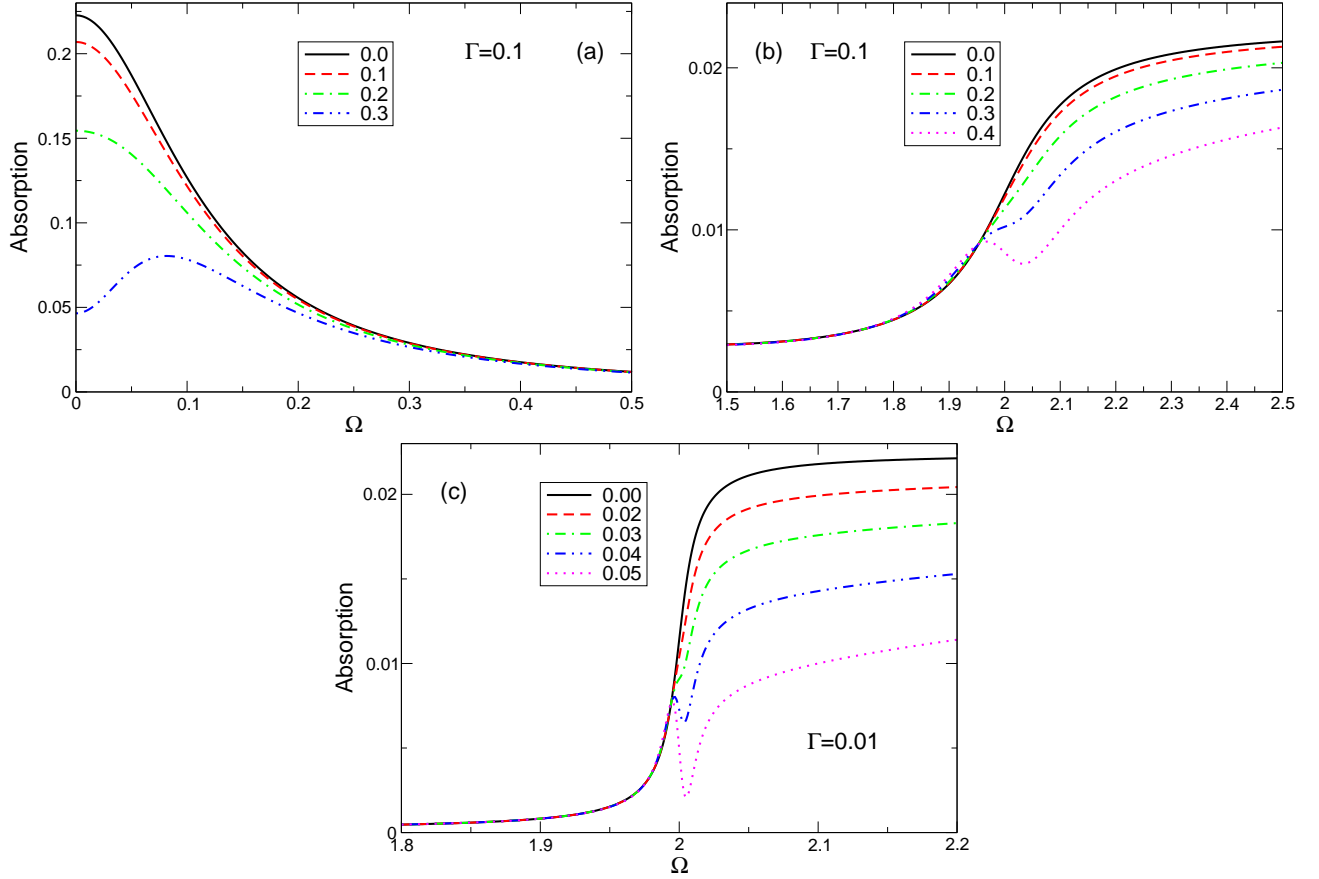


FIG. 9: The absorption coefficient in a single (isolated) graphene layer at (a) low and (b) high frequencies,  $\Gamma = 0.1$ , and (c) high frequencies at  $\Gamma = 0.01$ . The curves are labeled by the value of the dimensionless electric field  $eE_0/E_F k_F$ .

on the scattering rate  $\Gamma$ . If  $\Gamma \simeq 0.1$ , the absorption is noticeably suppressed at  $eE_0/E_F k_F$  of order of  $0.1 - 0.3$ . At the electron density  $n_s \simeq 10^{12} \text{ cm}^{-2}$  this corresponds to the electric fields

$$E_0 \simeq (0.1 - 0.3) \frac{\hbar v_F \pi n_s}{e} \simeq (20 - 60) \text{ kV/cm.} \quad (138)$$

If  $\Gamma$  is ten times smaller, Figure 9(c), the required electric field is reduced by, roughly, one order of magnitude. It is worth noting that at small values of  $\Gamma$  the resonance near  $\Omega \simeq 2$  is very narrow which can be used for a precise control of the saturable absorption of infrared- and visible-laser mirrors, cf.<sup>45,46</sup>.

## VII. DC CURRENT INDUCED SECOND HARMONIC GENERATION

Finally consider the system response to a monochromatic irradiation with the frequency  $\omega$  and a dc field  $E_0$ . Under these conditions the system is able to generate the second harmonic electromagnetic wave at the frequency  $2\omega$  since the applied dc current violates the central symmetry of graphene. Assume that both the dc and the ac fields are polarized in the same ( $x$ -) direction. Then

$$E_\alpha(t) = \delta_{\alpha x}(E_0 + E_1 \cos \omega t), \quad (139)$$

so that

$$E_{\omega_1}^\beta = \delta_{\beta x} \left[ E_0 \delta(\omega_1) + \frac{E_1}{2} \left( \delta(\omega_1 - \omega) + \delta(\omega_1 + \omega) \right) \right]. \quad (140)$$

The contribution to the current which corresponds to the oscillations with the frequency  $2\omega$  has the form

$$j_{x,2\omega}^{(3)}(t) = \frac{3}{4} E_0 E_1^2 \sigma_{xxxx}^{(3)}(\omega, \omega, 0) e^{-i2\omega t} + c.c. \quad (141)$$

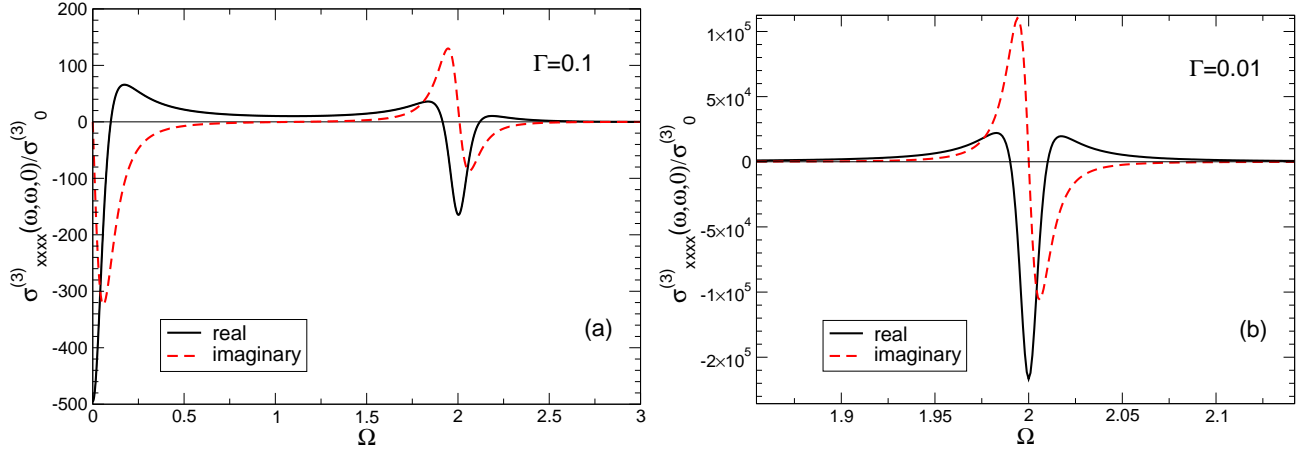


FIG. 10: The third-order conductivity  $\sigma_{xxxx}(\omega, \omega, 0)/\sigma_0^{(3)}$  as a function of frequency  $\Omega$  at (a)  $\Gamma = 0.1$  and (b)  $\Gamma = 0.01$  in the high-frequency range ( $\Omega \simeq 2$ ).

The function  $\sigma_{xxxx}^{(3)}(\omega, \omega, 0)$  is shown in Fig. 10. Notice that the height of the high-frequency resonance is only about five times smaller than that of the low-frequency resonance at  $\Gamma = 0.1$  which is substantially larger than in the case of the third-harmonic generation, cf. Fig. 4. It is also remarkable that the amplitude of the second harmonic is strongly influenced by the scattering parameter, see Fig. 10(b): the reduction of  $\Gamma$  by a factor of ten leads to the growth of  $\sigma_{xxxx}^{(3)}(\omega, \omega, 0)$  at  $\Omega \simeq 2$  by more than three orders of magnitude. The intensity of the second harmonic would then increase by more than six orders. The dc-current induced second harmonic generation can thus be used for different frequency-conversion devices operating both at terahertz and infrared/optical frequencies. The opportunity to use both third and (dc-current assisted) second harmonics essentially enhances the functionality of potential graphene based nonlinear devices.

### VIII. SUMMARY AND CONCLUSIONS

In this paper we have developed a full quantum theory of the third-order nonlinear electrodynamic response of graphene. The analytically calculated third-order conductivity  $\sigma_{\alpha\beta\gamma\delta}(\omega_1, \omega_2, \omega_3)$  can be used for analysis of a very large number of different nonlinear phenomena. Some of them have been investigated in this paper; other, such as the four wave mixing, dc current induced sum and difference generation, response to a pulse excitation will be studied in subsequent publications.

Our results show that there are two main frequency ranges where the nonlinear effects in graphene are especially large. The first range corresponds to the condition  $\Omega \lesssim \Gamma$ , or  $\omega\tau \lesssim 1$ , where  $\tau$  is the effective scattering time. In currently available graphene samples the time  $\tau$  lies in the range  $0.1 - 1$  ps meaning that the low-frequency range of strong nonlinear phenomena in graphene covers the technologically important range of microwave and terahertz frequencies  $f \lesssim 10$  THz.

At higher frequencies the nonlinear parameters strongly decrease with the frequency (as  $1/\omega^3$  at  $\hbar\omega \lesssim 2E_F$  and as  $1/\omega^4$  at  $\hbar\omega \gtrsim 2E_F$ ). Fortunately, in graphene the nonlinear response functions have a strong resonance around the frequency  $\hbar\omega \simeq 2E_F$ , where the nonlinear parameters of graphene are increased by orders of magnitude. The position of this resonance depends on the electron density and can therefore be electrically tuned from  $\sim 10$  to  $\sim 300$  THz (the wavelength from  $\sim 1$  to  $\sim 30$   $\mu$ m) thus opening a lot of interesting opportunities for creation of new innovative tunable devices operating across the terahertz through near-IR and visible frequency range.

The author thanks Yuri Kivshar and Mikhail Glazov for interesting discussions of theoretical issues, Nadja Savostianova for assistance, and Costantino de Angelis, Shakil Awan, Giulio Cerullo, Jérôme Faist, Andrea Ferrari, Jonathan Finley, Alexander Grigorenko, Samuel Ver Hoeye, Junichiro Kono, Antonio Lombardo, Geoffrey Nash, Daniel Popa and Hua Qin for interest and useful discussions related to possible experimental observations of the predicted effects. The work was supported by the European Union under the Program Graphene Flagship (No. CNECT-ICT-604391).

## Appendix A: Some useful formulas

Some definitions and formulas used in the main text are presented here. The two-dimensional Levi-Civita symbol is defined as

$$\epsilon_{\alpha\beta} = \begin{pmatrix} 0 & 1 \\ -1 & 0 \end{pmatrix}. \quad (\text{A1})$$

It satisfies the following relations:

$$\epsilon_{\alpha\mu}\epsilon_{\beta\nu} = \delta_{\alpha\beta}\delta_{\mu\nu} - \delta_{\alpha\nu}\delta_{\mu\beta}, \quad (\text{A2})$$

$$\epsilon_{\alpha\mu}\epsilon_{\beta\nu}\delta_{\mu\nu} = \epsilon_{\alpha\nu}\epsilon_{\beta\nu} = \delta_{\alpha\beta}. \quad (\text{A3})$$

$$\epsilon_{\alpha\lambda}\epsilon_{\beta\mu}\epsilon_{\gamma\nu}\epsilon_{\delta\sigma} \left( \delta_{\lambda\mu}\delta_{\nu\sigma} + \delta_{\lambda\nu}\delta_{\mu\sigma} + \delta_{\lambda\sigma}\delta_{\mu\nu} \right) = \delta_{\alpha\beta}\delta_{\gamma\delta} + \delta_{\alpha\gamma}\delta_{\beta\delta} + \delta_{\alpha\delta}\delta_{\beta\gamma}. \quad (\text{A4})$$

The integration over the polar angle in the  $\mathbf{k}$ -space is performed with the help of the formulas

$$\langle k_\alpha k_\beta \rangle \equiv \frac{1}{2\pi} \int_{-\pi}^{\pi} k_\alpha k_\beta d\phi = \frac{k^2}{2} \delta_{\alpha\beta}, \quad (\text{A5})$$

$$\langle k_\alpha k_\beta k_\gamma k_\delta \rangle \equiv \frac{1}{2\pi} \int_{-\pi}^{\pi} k_\alpha k_\beta k_\gamma k_\delta d\phi = \frac{k^4}{8} \left( \delta_{\alpha\beta}\delta_{\gamma\delta} + \delta_{\alpha\gamma}\delta_{\beta\delta} + \delta_{\alpha\delta}\delta_{\beta\gamma} \right). \quad (\text{A6})$$

## Appendix B: Transformation of formulas (55) and (56)

In this Section we show how one can transform (simplify) the formulas of the type (53) – (56) and simplify two of them, Eqs. (55) and (56).

### 1. Transformation of the $(1/2)$ term

First, we rewrite Eq. (55) in the form

$$\underbrace{j_\alpha^{(3)}(t)}_{(1/2)} = \int_{-\infty}^{\infty} d\omega_1 \int_{-\infty}^{\infty} d\omega_2 \int_{-\infty}^{\infty} d\omega_3 E_{\omega_1}^\beta E_{\omega_2}^\gamma E_{\omega_3}^\delta e^{-i(\omega_1+\omega_2+\omega_3)t} \times \frac{1}{\omega_1 + i\gamma} \frac{ie^4 g_s}{4\hbar S} \sum_{l\mathbf{k}} \langle l\mathbf{k} | \hat{v}_\alpha | l\mathbf{k} \rangle \eta_{\mathbf{k}}^\gamma \eta_{\mathbf{k}}^\delta \frac{\partial(f_{l\mathbf{k}} - f_{\bar{l}\mathbf{k}})}{\partial k_\beta} \frac{1}{(E_{l\mathbf{k}} - E_{\bar{l}\mathbf{k}} + \hbar\omega_2 + i\hbar\gamma)(E_{\bar{l}\mathbf{k}} - E_{l\mathbf{k}} + \hbar\omega_3 + i\hbar\gamma)}, \quad (\text{B1})$$

and present the product of two fractions as a sum of fractions

$$\frac{1}{(E_{l\mathbf{k}} - E_{\bar{l}\mathbf{k}} + \hbar\omega_2 + i\hbar\gamma)(E_{\bar{l}\mathbf{k}} - E_{l\mathbf{k}} + \hbar\omega_3 + i\hbar\gamma)} = \frac{1}{\hbar\omega_2 + \hbar\omega_3 + i2\hbar\gamma} \left( \frac{1}{E_{l\mathbf{k}} - E_{\bar{l}\mathbf{k}} + \hbar\omega_2 + i\hbar\gamma} + \frac{1}{E_{\bar{l}\mathbf{k}} - E_{l\mathbf{k}} + \hbar\omega_3 + i\hbar\gamma} \right). \quad (\text{B2})$$

This gives

$$\underbrace{j_\alpha^{(3)}(t)}_{(1/2)} = \int_{-\infty}^{\infty} d\omega_1 \int_{-\infty}^{\infty} d\omega_2 \int_{-\infty}^{\infty} d\omega_3 E_{\omega_1}^\beta E_{\omega_2}^\gamma E_{\omega_3}^\delta e^{-i(\omega_1+\omega_2+\omega_3)t} \frac{1}{\omega_1 + i\gamma} \frac{1}{\omega_2 + \omega_3 + i2\gamma} \times \frac{ie^4 g_s}{4\hbar^2 S} \left( \sum_{l\mathbf{k}} \frac{\langle l\mathbf{k} | \hat{v}_\alpha | l\mathbf{k} \rangle \eta_{\mathbf{k}}^\gamma \eta_{\mathbf{k}}^\delta}{E_{l\mathbf{k}} - E_{\bar{l}\mathbf{k}} + \hbar\omega_2 + i\hbar\gamma} \frac{\partial(f_{l\mathbf{k}} - f_{\bar{l}\mathbf{k}})}{\partial k_\beta} + \sum_{l\mathbf{k}} \frac{\langle l\mathbf{k} | \hat{v}_\alpha | l\mathbf{k} \rangle \eta_{\mathbf{k}}^\gamma \eta_{\mathbf{k}}^\delta}{E_{\bar{l}\mathbf{k}} - E_{l\mathbf{k}} + \hbar\omega_3 + i\hbar\gamma} \frac{\partial(f_{l\mathbf{k}} - f_{\bar{l}\mathbf{k}})}{\partial k_\beta} \right). \quad (\text{B3})$$

Replacing the summation index  $l \leftrightarrow \bar{l}$  in the first term and permuting  $(\gamma, \omega_2) \leftrightarrow (\delta, \omega_3)$  in the second one we obtain

$$\underbrace{j_{\alpha}^{(3)}(t)}_{(1/2)} = \int_{-\infty}^{\infty} d\omega_1 \int_{-\infty}^{\infty} d\omega_2 \int_{-\infty}^{\infty} d\omega_3 E_{\omega_1}^{\beta} E_{\omega_2}^{\gamma} E_{\omega_3}^{\delta} e^{-i(\omega_1+\omega_2+\omega_3)t} \frac{1}{\omega_1 + i\gamma} \frac{1}{\omega_2 + \omega_3 + i2\gamma} \times \frac{ie^4 g_s}{4\hbar^2 S} \left( \sum_{l\mathbf{k}} \frac{\langle \bar{l}\mathbf{k} | \hat{v}_{\alpha} | \bar{l}\mathbf{k} \rangle \eta_{\mathbf{k}}^{\gamma} \eta_{\mathbf{k}}^{\delta}}{E_{\bar{l}\mathbf{k}} - E_{l\mathbf{k}} + \hbar\omega_2 + i\hbar\gamma} \frac{\partial(f_{l\mathbf{k}} - f_{\bar{l}\mathbf{k}})}{\partial k_{\beta}} + \sum_{l\mathbf{k}} \frac{\langle l\mathbf{k} | \hat{v}_{\alpha} | l\mathbf{k} \rangle \eta_{\mathbf{k}}^{\gamma} \eta_{\mathbf{k}}^{\delta}}{E_{\bar{l}\mathbf{k}} - E_{l\mathbf{k}} + \hbar\omega_2 + i\hbar\gamma} \frac{\partial(f_{l\mathbf{k}} - f_{\bar{l}\mathbf{k}})}{\partial k_{\beta}} \right). \quad (\text{B4})$$

Since, according to (24),  $\langle \bar{l}\mathbf{k} | \hat{v}_{\alpha} | \bar{l}\mathbf{k} \rangle = -\langle l\mathbf{k} | \hat{v}_{\alpha} | l\mathbf{k} \rangle$ , we see that the two terms in the second line in (B4) are identical. This gives the formula (57) for the (1/2) current.

## 2. Transformation of the (0/3) term

Similarly, in order to transform Eq. (56) to a simpler form we rewrite it as follows

$$\underbrace{j_{\alpha}^{(3)}(t)}_{(0/3)} = \int_{-\infty}^{\infty} d\omega_1 \int_{-\infty}^{\infty} d\omega_2 \int_{-\infty}^{\infty} d\omega_3 E_{\omega_1}^{\beta} E_{\omega_2}^{\gamma} E_{\omega_3}^{\delta} e^{-i(\omega_1+\omega_2+\omega_3)t} \frac{ie^4 g_s}{4S} \sum_{l\mathbf{k}} \frac{\langle \bar{l}\mathbf{k} | \hat{v}_{\alpha} | l\mathbf{k} \rangle \eta_{\mathbf{k}}^{\beta} \eta_{\mathbf{k}}^{\gamma} \eta_{\mathbf{k}}^{\delta} (f_{l\mathbf{k}} - f_{\bar{l}\mathbf{k}})}{E_{\bar{l}\mathbf{k}} - E_{l\mathbf{k}} + \hbar(\omega_1 + \omega_2 + \omega_3) + i\hbar 3\gamma} \times \frac{1}{(E_{\bar{l}\mathbf{k}} - E_{l\mathbf{k}} + \hbar\omega_1 + i\hbar\gamma)(E_{\bar{l}\mathbf{k}} - E_{l\mathbf{k}} + \hbar\omega_2 + i\hbar\gamma)} \quad (\text{B5})$$

and present the product of two fractions in the second line as a sum of two fractions:

$$\begin{aligned} & \frac{1}{(E_{\bar{l}\mathbf{k}} - E_{l\mathbf{k}} + \hbar\omega_1 + i\hbar\gamma)(E_{\bar{l}\mathbf{k}} - E_{l\mathbf{k}} + \hbar\omega_2 + i\hbar\gamma)} \\ &= \frac{1}{\hbar\omega_1 + \hbar\omega_2 + i2\hbar\gamma} \left( \frac{1}{E_{\bar{l}\mathbf{k}} - E_{l\mathbf{k}} + \hbar\omega_1 + i\hbar\gamma} + \frac{1}{E_{\bar{l}\mathbf{k}} - E_{l\mathbf{k}} + \hbar\omega_2 + i\hbar\gamma} \right). \end{aligned} \quad (\text{B6})$$

The substitution of (B6) back to (B5) gives

$$\begin{aligned} \underbrace{j_{\alpha}^{(3)}(t)}_{(0/3)} &= \int_{-\infty}^{\infty} d\omega_1 \int_{-\infty}^{\infty} d\omega_2 \int_{-\infty}^{\infty} d\omega_3 E_{\omega_1}^{\beta} E_{\omega_2}^{\gamma} E_{\omega_3}^{\delta} e^{-i(\omega_1+\omega_2+\omega_3)t} \frac{ie^4 g_s}{4\hbar S} \frac{1}{\omega_1 + \omega_2 + i2\gamma} \\ &\times \left( \sum_{l\mathbf{k}} \frac{\langle \bar{l}\mathbf{k} | \hat{v}_{\alpha} | l\mathbf{k} \rangle \eta_{\mathbf{k}}^{\beta} \eta_{\mathbf{k}}^{\gamma} \eta_{\mathbf{k}}^{\delta} (f_{l\mathbf{k}} - f_{\bar{l}\mathbf{k}})}{E_{\bar{l}\mathbf{k}} - E_{l\mathbf{k}} + \hbar(\omega_1 + \omega_2 + \omega_3) + i\hbar 3\gamma} \frac{1}{E_{\bar{l}\mathbf{k}} - E_{l\mathbf{k}} + \hbar\omega_1 + i\hbar\gamma} \right. \\ &\left. + \sum_{l\mathbf{k}} \frac{\langle \bar{l}\mathbf{k} | \hat{v}_{\alpha} | l\mathbf{k} \rangle \eta_{\mathbf{k}}^{\beta} \eta_{\mathbf{k}}^{\gamma} \eta_{\mathbf{k}}^{\delta} (f_{l\mathbf{k}} - f_{\bar{l}\mathbf{k}})}{E_{\bar{l}\mathbf{k}} - E_{l\mathbf{k}} + \hbar(\omega_1 + \omega_2 + \omega_3) + i\hbar 3\gamma} \frac{1}{E_{\bar{l}\mathbf{k}} - E_{l\mathbf{k}} + \hbar\omega_2 + i\hbar\gamma} \right). \end{aligned} \quad (\text{B7})$$

Now we replace  $(\beta, \omega_1) \leftrightarrow (\gamma, \omega_2)$  in the last term (the third line). This permutation leads only to the replacement  $\omega_2 \rightarrow \omega_1$  in the very last fraction  $(E_{l\mathbf{k}} - E_{\bar{l}\mathbf{k}} + \hbar\omega_2 + i\hbar\gamma)^{-1}$ , since in all other places the indexes  $\beta, \gamma$  and the frequencies  $\omega_1, \omega_2$  enter symmetrically. So we get

$$\begin{aligned} \underbrace{j_{\alpha}^{(3)}(t)}_{(0/3)} &= \int_{-\infty}^{\infty} d\omega_1 \int_{-\infty}^{\infty} d\omega_2 \int_{-\infty}^{\infty} d\omega_3 E_{\omega_1}^{\beta} E_{\omega_2}^{\gamma} E_{\omega_3}^{\delta} e^{-i(\omega_1+\omega_2+\omega_3)t} \frac{ie^4 g_s}{4\hbar S} \frac{1}{\omega_1 + \omega_2 + i2\gamma} \\ &\times \left( \sum_{l\mathbf{k}} \frac{\langle \bar{l}\mathbf{k} | \hat{v}_{\alpha} | l\mathbf{k} \rangle \eta_{\mathbf{k}}^{\beta} \eta_{\mathbf{k}}^{\gamma} \eta_{\mathbf{k}}^{\delta} (f_{l\mathbf{k}} - f_{\bar{l}\mathbf{k}})}{E_{\bar{l}\mathbf{k}} - E_{l\mathbf{k}} + \hbar(\omega_1 + \omega_2 + \omega_3) + i\hbar 3\gamma} \frac{1}{E_{\bar{l}\mathbf{k}} - E_{l\mathbf{k}} + \hbar\omega_1 + i\hbar\gamma} \right. \\ &\left. + \sum_{l\mathbf{k}} \frac{\langle \bar{l}\mathbf{k} | \hat{v}_{\alpha} | l\mathbf{k} \rangle \eta_{\mathbf{k}}^{\beta} \eta_{\mathbf{k}}^{\gamma} \eta_{\mathbf{k}}^{\delta} (f_{l\mathbf{k}} - f_{\bar{l}\mathbf{k}})}{E_{\bar{l}\mathbf{k}} - E_{l\mathbf{k}} + \hbar(\omega_1 + \omega_2 + \omega_3) + i\hbar 3\gamma} \frac{1}{E_{\bar{l}\mathbf{k}} - E_{l\mathbf{k}} + \hbar\omega_2 + i\hbar\gamma} \right). \end{aligned} \quad (\text{B8})$$

The third-line term in (B8) differs from the second-line term only by the energy difference in the last fraction,  $E_{\bar{l}\mathbf{k}} - E_{l\mathbf{k}}$  vs.  $E_{l\mathbf{k}} - E_{\bar{l}\mathbf{k}}$ . Transforming the products of the fractions by their difference (in the second-line term) and by their

sum (in the third-line term) we get

$$\begin{aligned}
\underbrace{j_{\alpha}^{(3)}(t)}_{(0/3)} &= \int_{-\infty}^{\infty} d\omega_1 \int_{-\infty}^{\infty} d\omega_2 \int_{-\infty}^{\infty} d\omega_3 E_{\omega_1}^{\beta} E_{\omega_2}^{\gamma} E_{\omega_3}^{\delta} e^{-i(\omega_1+\omega_2+\omega_3)t} \frac{ie^4 g_s}{4\hbar S} \frac{1}{\omega_1 + \omega_2 + i2\gamma} \\
&\times \left( \sum_{l\mathbf{k}} \langle \bar{l}\mathbf{k} | \hat{v}_{\alpha} | l\mathbf{k} \rangle \eta_{\mathbf{k}}^{\beta} \eta_{\mathbf{k}}^{\gamma} \eta_{\mathbf{k}}^{\delta} (f_{l\mathbf{k}} - f_{\bar{l}\mathbf{k}}) \frac{-1}{\hbar(\omega_2 + \omega_3) + i\hbar 2\gamma} \right. \\
&\times \left( \frac{1}{E_{\bar{l}\mathbf{k}} - E_{l\mathbf{k}} + \hbar(\omega_1 + \omega_2 + \omega_3) + i\hbar 3\gamma} - \frac{1}{E_{\bar{l}\mathbf{k}} - E_{l\mathbf{k}} + \hbar\omega_1 + i\hbar\gamma} \right) \\
&+ \sum_{l\mathbf{k}} \langle \bar{l}\mathbf{k} | \hat{v}_{\alpha} | l\mathbf{k} \rangle \eta_{\mathbf{k}}^{\beta} \eta_{\mathbf{k}}^{\gamma} \eta_{\mathbf{k}}^{\delta} (f_{l\mathbf{k}} - f_{\bar{l}\mathbf{k}}) \frac{1}{\hbar(2\omega_1 + \omega_2 + \omega_3) + i\hbar 4\gamma} \\
&\times \left. \left( \frac{1}{E_{\bar{l}\mathbf{k}} - E_{l\mathbf{k}} + \hbar(\omega_1 + \omega_2 + \omega_3) + i\hbar 3\gamma} + \frac{1}{E_{l\mathbf{k}} - E_{\bar{l}\mathbf{k}} + \hbar\omega_1 + i\hbar\gamma} \right) \right) \\
&= \int_{-\infty}^{\infty} d\omega_1 \int_{-\infty}^{\infty} d\omega_2 \int_{-\infty}^{\infty} d\omega_3 E_{\omega_1}^{\beta} E_{\omega_2}^{\gamma} E_{\omega_3}^{\delta} e^{-i(\omega_1+\omega_2+\omega_3)t} \frac{ie^4 g_s}{4\hbar^2 S} \frac{1}{\omega_1 + \omega_2 + i2\gamma} \\
&\times \left( -\frac{1}{\omega_2 + \omega_3 + i2\gamma} \left( \sum_{l\mathbf{k}} \frac{\langle \bar{l}\mathbf{k} | \hat{v}_{\alpha} | l\mathbf{k} \rangle \eta_{\mathbf{k}}^{\beta} \eta_{\mathbf{k}}^{\gamma} \eta_{\mathbf{k}}^{\delta} (f_{l\mathbf{k}} - f_{\bar{l}\mathbf{k}})}{E_{\bar{l}\mathbf{k}} - E_{l\mathbf{k}} + \hbar(\omega_1 + \omega_2 + \omega_3) + i\hbar 3\gamma} - \sum_{l\mathbf{k}} \frac{\langle \bar{l}\mathbf{k} | \hat{v}_{\alpha} | l\mathbf{k} \rangle \eta_{\mathbf{k}}^{\beta} \eta_{\mathbf{k}}^{\gamma} \eta_{\mathbf{k}}^{\delta} (f_{l\mathbf{k}} - f_{\bar{l}\mathbf{k}})}{E_{l\mathbf{k}} - E_{\bar{l}\mathbf{k}} + \hbar\omega_1 + i\hbar\gamma} \right) \right. \\
&+ \left. \frac{1}{2\omega_1 + \omega_2 + \omega_3 + i4\gamma} \left( \sum_{l\mathbf{k}} \frac{\langle \bar{l}\mathbf{k} | \hat{v}_{\alpha} | l\mathbf{k} \rangle \eta_{\mathbf{k}}^{\beta} \eta_{\mathbf{k}}^{\gamma} \eta_{\mathbf{k}}^{\delta} (f_{l\mathbf{k}} - f_{\bar{l}\mathbf{k}})}{E_{\bar{l}\mathbf{k}} - E_{l\mathbf{k}} + \hbar(\omega_1 + \omega_2 + \omega_3) + i\hbar 3\gamma} + \sum_{l\mathbf{k}} \frac{\langle \bar{l}\mathbf{k} | \hat{v}_{\alpha} | l\mathbf{k} \rangle \eta_{\mathbf{k}}^{\beta} \eta_{\mathbf{k}}^{\gamma} \eta_{\mathbf{k}}^{\delta} (f_{l\mathbf{k}} - f_{\bar{l}\mathbf{k}})}{E_{l\mathbf{k}} - E_{\bar{l}\mathbf{k}} + \hbar\omega_1 + i\hbar\gamma} \right) \right). \tag{B9}
\end{aligned}$$

One sees that the sums with three omega's in the denominator ( $\omega_1 + \omega_2 + \omega_3$ ) are identical, while those with one omega ( $\omega_1$ ) differ by the summation index  $l$ . Replacing  $l$  by  $\bar{l}$  in the very last term we see that they are actually identical too (the product  $\langle \bar{l}\mathbf{k} | \hat{v}_{\alpha} | l\mathbf{k} \rangle (f_{l\mathbf{k}} - f_{\bar{l}\mathbf{k}})$  does not change after the replacement  $l \leftrightarrow \bar{l}$ ). Thus we get

$$\begin{aligned}
\underbrace{j_{\alpha}^{(3)}(t)}_{(0/3)} &= \int_{-\infty}^{\infty} d\omega_1 \int_{-\infty}^{\infty} d\omega_2 \int_{-\infty}^{\infty} d\omega_3 E_{\omega_1}^{\beta} E_{\omega_2}^{\gamma} E_{\omega_3}^{\delta} e^{-i(\omega_1+\omega_2+\omega_3)t} \frac{1}{2} \frac{1}{\omega_1 + \omega_2 + i2\gamma} \\
&\times \left( \frac{\mathcal{F}(\omega_1 + \omega_2 + \omega_3 + i3\gamma) + \mathcal{F}(\omega_1 + i\gamma)}{2\omega_1 + \omega_2 + \omega_3 + i4\gamma} - \frac{\mathcal{F}(\omega_1 + \omega_2 + \omega_3 + i3\gamma) - \mathcal{F}(\omega_1 + i\gamma)}{\omega_2 + \omega_3 + i2\gamma} \right), \tag{B10}
\end{aligned}$$

where the function  $\mathcal{F}$  is defined in (59). Rearranging the terms in (B10) we finally obtain the formula (58) from the main text.

---

\* Electronic mail: sergey.mikhailov@physik.uni-augsburg.de

<sup>1</sup> F. Bonaccorso, Z. Sun, T. Hasan, and A. C. Ferrari, *Nature Photonics* **4**, 611 (2010).

<sup>2</sup> R. R. Hartmann, J. Kono, and M. E. Portnoi, *Nanotechnology* **25**, 322001 (2014).

<sup>3</sup> M. M. Glazov and S. Ganichev, *Phys. Rep.* **535**, 101 (2014).

<sup>4</sup> A. C. Ferrari, F. Bonaccorso, V. Fal'ko, K. S. Novoselov, S. Roche, P. Boggild, S. Borini, F. H. L. Koppens, V. Palermo, N. Pugno, et al., *Nanoscale* **7**, 4598 (2015), URL <http://dx.doi.org/10.1039/C4NR01600A>.

<sup>5</sup> E. A. Henriksen, Z. Jiang, L. C. Tung, M. E. Schwartz, M. Takita, Y.-J. Wang, P. Kim, and H. L. Stormer, *Phys. Rev. Lett.* **100**, 087403 (2008).

<sup>6</sup> V. P. Gusynin, S. G. Sharapov, and J. P. Carbotte, *Phys. Rev. Lett.* **98**, 157402 (2007).

<sup>7</sup> L. A. Falkovsky and A. A. Varlamov, *Europ. Phys. J. B* **56**, 281 (2007).

<sup>8</sup> S. A. Mikhailov and K. Ziegler, *Phys. Rev. Lett.* **99**, 016803 (2007).

<sup>9</sup> B. Wunsch, T. Stauber, F. Sols, and F. Guinea, *New J. Phys.* **8**, 318 (2006).

<sup>10</sup> E. H. Hwang and S. Das Sarma, *Phys. Rev. B* **75**, 205418 (2007).

<sup>11</sup> A. Bostwick, T. Ohta, T. Seyller, K. Horn, and E. Rotenberg, *Nature Physics* **3**, 36 (2007).

<sup>12</sup> V. Ryzhii, A. Satou, and T. Otsuji, *J. Appl. Phys.* **101**, 024509 (2007).

<sup>13</sup> A. B. Kuzmenko, E. van Heumen, F. Carbone, and D. van der Marel, *Phys. Rev. Lett.* **100**, 117401 (2008).

<sup>14</sup> R. R. Nair, P. Blake, A. N. Grigorenko, K. S. Novoselov, T. J. Booth, T. Stauber, N. M. R. Peres, and A. K. Geim, *Science* **320**, 1308 (2008).

<sup>15</sup> N. M. R. Peres, T. Stauber, and A. H. Castro Neto, *Europhys. Lett.* **84**, 38002 (2008).

<sup>16</sup> Z. Q. Li, E. A. Henriksen, Z. Jiang, Z. Hao, M. C. Martin, P. Kim, H. L. Stormer, and D. N. Basov, *Nature Physics* **4**, 532 (2008).

<sup>17</sup> K. F. Mak, M. Y. Sfeir, Y. Wu, C. H. Lui, J. A. Misewich, and T. F. Heinz, *Phys. Rev. Lett.* **101**, 196405 (2008).

<sup>18</sup> Z. Sun, T. Hasan, F. Torrisi, D. Popa, G. Privitera, F. Wang, F. Bonaccorso, D. M. Basko, and A. C. Ferrari, *ACS Nano* **4**, 803 (2010).

<sup>19</sup> S. A. Mikhailov, *Europhys. Lett.* **79**, 27002 (2007).

<sup>20</sup> M. Dragoman, D. Neculoiu, G. Deligeorgis, G. Konstantinidis, D. Dragoman, A. Cismaru, A. A. Muller, and R. Plana, *Appl. Phys. Lett.* **97**, 093101 (2010).

<sup>21</sup> E. Hendry, P. J. Hale, J. J. Moger, A. K. Savchenko, and S. A. Mikhailov, *Phys. Rev. Lett.* **105**, 097401 (2010).

<sup>22</sup> S. A. Mikhailov and K. Ziegler, *J. Phys. Condens. Matter* **20**, 384204 (2008).

<sup>23</sup> S. A. Mikhailov, *Physica E* **40**, 2626 (2008).

<sup>24</sup> S. A. Mikhailov, *Microelectron. J.* **40**, 712 (2009).

<sup>25</sup> S. A. Mikhailov, in *Physics and Applications of Graphene: Theory*, edited by S. A. Mikhailov (InTech, Rijeka, Croatia, 2011), chap. 25, pp. 519–534, ISBN: 978-953-307-152-7.

<sup>26</sup> S. A. Mikhailov, *Phys. Rev. B* **84**, 045432 (2011).

<sup>27</sup> S. A. Mikhailov, *Physica E* **44**, 924 (2012).

<sup>28</sup> S. A. Mikhailov, *Phys. Rev. B* **90**, 241301(R) (2014), *Phys. Rev. B*, **91**, 039904(E) (2015).

<sup>29</sup> D. A. Smirnova, I. V. Shadrivov, A. E. Miroshnichenko, A. I. Smirnov, and Y. S. Kivshar, *Phys. Rev. B* **90**, 035412 (2014), URL <http://link.aps.org/doi/10.1103/PhysRevB.90.035412>.

<sup>30</sup> X. Yao, M. Tokman, and A. Belyanin, *Phys. Rev. Lett.* **112**, 055501 (2014).

<sup>31</sup> N. M. R. Peres, Y. V. Bludov, J. E. Santos, A.-P. Jauho, and M. I. Vasilevskiy, *Phys. Rev. B* **90**, 125425 (2014).

<sup>32</sup> J. L. Cheng, N. Vermeulen, and J. E. Sipe, *New J. Phys.* **16**, 053014 (2014).

<sup>33</sup> J. L. Cheng, N. Vermeulen, and J. E. Sipe, *Optics Express* **22**, 15868 (2014).

<sup>34</sup> J. L. Cheng, N. Vermeulen, and J. E. Sipe (2015), arXiv:1503.07564.

<sup>35</sup> J. J. Dean and H. M. van Driel, *Appl. Phys. Lett.* **95**, 261910 (2009).

<sup>36</sup> J. J. Dean and H. M. van Driel, *Phys. Rev. B* **82**, 125411 (2010).

<sup>37</sup> R. Wu, Y. Zhang, S. Yan, F. Bian, W. Wang, X. Bai, X. Lu, J. Zhao, and E. Wang, *Nano Lett.* **11**, 51595164 (2011).

<sup>38</sup> T. Gu, N. Petrone, J. F. McMillan, A. van der Zande, M. Yu, G. Q. Lo, D. L. Kwong, J. Hone, and C. W. Wong, *Nature Photonics* **6**, 554559 (2012).

<sup>39</sup> H. Zhang, S. Virally, Q. Bao, L. K. Ping, S. Massar, N. Godbout, and P. Kockaert, *Optics Letters* **37**, 1856 (2012).

<sup>40</sup> A. Y. Bykov, T. V. Murzina, M. G. Rybin, and E. D. Obraztsova, *Phys. Rev. B* **85**, 121413(R) (2012).

<sup>41</sup> N. Kumar, J. Kumar, C. Gerstenkorn, R. Wang, H.-Y. Chiu, A. L. Smirl, and H. Zhao, *Phys. Rev. B* **87**, 121406(R) (2013).

<sup>42</sup> S.-Y. Hong, J. I. Dadap, N. Petrone, P.-C. Yeh, J. Hone, and R. M. Osgood, Jr., *Phys. Rev. X* **3**, 021014 (2013).

<sup>43</sup> Y. Q. An, J. E. Rowe, D. B. Dougherty, J. U. Lee, and A. C. Diebold, *Phys. Rev. B* **89**, 115310 (2014).

<sup>44</sup> K.-H. Lin, S.-W. Weng, P.-W. Lyu, T.-R. Tsai, and W.-B. Su, *Appl. Phys. Lett.* **76**, 151605 (2014).

<sup>45</sup> D. Popa, Z. Sun, F. Torrisi, T. Hasan, F. Wang, and A. C. Ferrari, *Appl. Phys. Lett.* **97**, 203106 (2010).

<sup>46</sup> D. Popa, Z. Sun, T. Hasan, F. Torrisi, F. Wang, and A. C. Ferrari, *Appl. Phys. Lett.* **98**, 073106 (2011).